

Coordinate-Descent Diffusion Learning by Networked Agents

Chengcheng Wang, *Student Member, IEEE*, Yonggang Zhang, *Senior Member, IEEE*,
Bicheng Ying, *Student Member, IEEE*, and Ali H. Sayed, *Fellow, IEEE*

Abstract—This work examines the mean-square error performance of diffusion stochastic algorithms under a generalized coordinate-descent scheme. In this setting, the adaptation step by each agent is limited to a random subset of the coordinates of its stochastic gradient vector. The selection of coordinates varies randomly from iteration to iteration and from agent to agent across the network. Such schemes are useful in reducing computational complexity at each iteration in power-intensive large data applications. They are also useful in modeling situations where some partial gradient information may be missing at random. Interestingly, the results show that the steady-state performance of the learning strategy is not always degraded, while the convergence rate suffers some degradation. The results provide yet another indication of the resilience and robustness of adaptive distributed strategies.

Index Terms—Coordinate descent, stochastic partial update, computational complexity, diffusion strategies, stochastic gradient algorithms, strongly-convex cost.

I. INTRODUCTION AND RELATED WORK

Consider a strongly-connected network of N agents, where information can flow in either direction between any two connected agents and, moreover, there is at least one self-loop in the topology [2, p. 436]. We associate a strongly convex differentiable risk, $J_k(w)$, with each agent k and assume in this work that all these costs share a common minimizer, $w^o \in \mathbb{R}^M$, where \mathbb{R} denotes field of real numbers. This case models important situations where agents work cooperatively towards the same goal. The objective of the network is to determine the unique minimizer w^o of the following aggregate cost, assumed to be strongly-convex:

$$J^{\text{glob}}(w) \triangleq \sum_{k=1}^N J_k(w) \quad (1)$$

A short version of this work appears in the conference publication [1].

This work was performed while C. Wang was a visiting student at the UCLA Adaptive Systems Laboratory. The work of C. Wang was supported in part by a Chinese Government Scholarship. The work of Y. Zhang was supported in part by the National Natural Science Foundation of China (61371173), and Fundamental Research Funds for the Central University of Harbin Engineering University (HEUCFP201705). The work of B. Ying and A. H. Sayed was supported in part by NSF grants CCF-1524250 and ECCS-1407712.

C. Wang and Y. Zhang are with the College of Automation, Harbin Engineering University, Harbin, Heilongjiang 150001 China. C. Wang is also with the School of Electrical and Electronic Engineering, Nanyang Technological University, 639798 Singapore (e-mail: wangcc@ntu.edu.sg; zhangyg@hrbeu.edu.cn).

B. Ying is with the Department of Electrical Engineering, University of California, Los Angeles, CA 90024 USA (e-mail: ybc@ucla.edu).

A. H. Sayed is with the Ecole Polytechnique Federale de Lausanne, EPFL, School of Engineering, CH-1015 Lausanne, Switzerland (e-mail: ali.sayed@epfl.ch).

It is also assumed that the individual cost functions, $J_k(w)$, are each twice-differentiable and satisfy

$$0 < \nu_d I_M \leq \nabla_w^2 J_k(w) \leq \delta_d I_M \quad (2)$$

where $\nabla_w^2 J_k(w)$ denotes the $M \times M$ Hessian matrix of $J_k(w)$ with respect to w , $\nu_d \leq \delta_d$ are positive parameters, and I_M is the $M \times M$ identity matrix. In addition, for matrices A and B , the notation $A \leq B$ denotes that $B - A$ is positive semi-definite. The condition in (2) is automatically satisfied by important cases of interest, such as logistic regression or mean-square-error designs [2], [3].

Starting from some initial conditions $\{w_{k,-1}\}$, the agents work cooperatively in an adaptive manner to seek the minimizer w^o of problem (1) by applying the following diffusion strategy [2], [3]:

$$\begin{cases} \phi_{k,i-1} = \sum_{\ell \in \mathcal{N}_k} a_{1,\ell k} w_{\ell,i-1} & (3a) \\ \psi_{k,i} = \phi_{k,i-1} - \mu_k \widehat{\nabla_{w^\top} J_k}(\phi_{k,i-1}) & (3b) \\ w_{k,i} = \sum_{\ell \in \mathcal{N}_k} a_{2,\ell k} \psi_{\ell,i} & (3c) \end{cases}$$

where the M -vector $w_{k,i}$ denotes the estimate by agent k at iteration i for w^o , while $\psi_{k,i}$ and $\phi_{k,i-1}$ are intermediate estimates. Moreover, an approximation for the true gradient vector of $J_k(w)$, $\widehat{\nabla_{w^\top} J_k}(\cdot)$, is used in (3b) since it is generally the case that the true gradient vector is not available (e.g., when $J_k(w)$ is defined as the expectation of some loss function and the probability distribution of the data is not known beforehand to enable computation of $J_k(\cdot)$ or its gradient vector). The symbol \mathcal{N}_k in (3) refers to the neighborhood of agent k . The $N \times N$ combination matrices $A_1 = [a_{1,\ell k}]$ and $A_2 = [a_{2,\ell k}]$ are left-stochastic matrices consisting of convex combination coefficients that satisfy:

$$a_{j,\ell k} \geq 0, \quad \sum_{\ell=1}^N a_{j,\ell k} = 1, \quad a_{j,\ell k} = 0, \text{ if } \ell \notin \mathcal{N}_k \quad (4)$$

for $j = 1, 2$. Either of these two matrices can be chosen as the identity matrix, in which case algorithm (3) reduces to one of two common forms for diffusion adaptation: the adapt-then-combine (ATC) form when $A_1 = I$ and the combine-then-adapt (CTA) form when $A_2 = I$. We continue to work with the general formulation (3) in order to treat both algorithms, and other cases as well, in a unified manner. The parameter $\mu_k > 0$ is a constant step-size factor used to drive the adaptation process. Its value is set to a constant in order to enable

continuous adaptation in response to streaming data or drifting minimizers. We could also consider a distributed implementation of the useful consensus-type [2], [4]–[11]. However, it has been shown in [2], [12] that when constant step-sizes are used to drive adaptation, the diffusion networks have wider stability ranges and superior performance. This is because consensus implementations have an inherent asymmetry in their updates, which can cause network graphs to behave in an unstable manner when the step-size is constant. This problem does not occur over diffusion networks. Since adaptation is a core element of the proposed strategies in this work, we therefore focus on diffusion learning mechanisms.

The main distinction in this work relative to prior studies on diffusion or consensus adaptive networks is that we now assume that, at each iteration i , the adaptation step in (3b) has only access to a *random subset* of the entries of the approximate gradient vector. This situation may arise due to missing data or a purposeful desire to reduce the computational burden of the update step. We model this scenario by replacing the approximate gradient vector by

$$\widehat{\nabla_{w^\top} J_k}^{\text{miss}}(\phi_{k,i-1}) = \Gamma_{k,i} \cdot \widehat{\nabla_{w^\top} J_k}(\phi_{k,i-1}) \quad (5)$$

where the random matrix $\Gamma_{k,i}$ is diagonal and consists of Bernoulli random variables $\{\mathbf{r}_{k,i}(m)\}$; each of these variables is either zero or one with probability

$$\text{Prob}(\mathbf{r}_{k,i}(m) = 0) \triangleq r_k \quad (6)$$

where $0 \leq r_k < 1$ and

$$\Gamma_{k,i} = \text{diag}\{\mathbf{r}_{k,i}(1), \mathbf{r}_{k,i}(2), \dots, \mathbf{r}_{k,i}(M)\} \quad (7)$$

In the case when $\mathbf{r}_{k,i}(m) = 0$, the m -th entry of the gradient vector is missing, and then the m -th entry of $\psi_{k,i}$ in (3b) is not updated. Observe that we are attaching two subscripts to \mathbf{r} : k and i , which means that we are allowing the randomness in the update to vary across agents and also over time.

A. Relation to Block-Coordinate Descent Methods

Our formulation provides a nontrivial generalization of the powerful random coordinate-descent technique studied, for example, in the context of deterministic optimization in [13]–[15] and the references therein. Random coordinate-descent has been primarily applied in the literature to single-agent convex optimization, namely, to problems of the form:

$$w^o = \arg \min_w J(w) \quad (8)$$

where $J(w)$ is assumed to be known beforehand. The traditional gradient descent algorithm for seeking the minimizer of $J(w)$, assumed differentiable, takes the form

$$w_i = w_{i-1} - \mu \nabla_{w^\top} J(w_{i-1}) \quad (9)$$

where the full gradient vector is used at every iteration to update w_{i-1} to w_i . In a coordinate-descent implementation, on the other hand, at every iteration i , only a subset of the entries of the gradient vector is used to perform the update. These subsets are usually chosen as follows. First, a collection of K partitions of the parameter space w is defined. These

partitions are defined by diagonal matrices, $\{\Omega_k\}$. Each matrix has ones and zeros on the diagonal and the matrices add up to the identity matrix:

$$\sum_{k=1}^K \Omega_k = I_M \quad (10)$$

Multiplying w by any Ω_k results in a vector of similar size, albeit one where the only nontrivial entries are those extracted by the unit locations in Ω_k . At every iteration i , one of the partitions is selected randomly, say, with probability

$$\text{Prob}(\Gamma_i = \Omega_k) = \omega_k \quad (11)$$

where the $\{\omega_k\}$ add up to one. Subsequently, the gradient descent iteration is replaced by

$$w_i = w_{i-1} - \mu \Gamma_i \nabla_{w^\top} J(w_{i-1}) \quad (12)$$

This formulation is known as the randomized block-coordinate descent (RBCD) algorithm [13]–[15]. At each iteration, the gradient descent step employs only a collection of coordinates represented by the selected entries from the gradient vector. Besides reducing complexity, this step helps alleviate the condition on the step-size parameter for convergence.

If we reduce our formulation (3)–(5) to the single agent case, it will become similar to (12) in that the desired cost function is optimized only along a *subset* of the coordinates at each iteration. However, our algorithm offers more randomness in generating the coordinate blocks than the RBCD algorithm, by allowing more random combinations of the coordinates at each time index. In particular, we do not limit the selection of the coordinates to a collection of K possibilities predetermined by the $\{\Omega_k\}$. Moreover, in our work we use a random subset of the *stochastic* gradient vector instead of the *true* gradient vector to update the estimate, which is necessary for adaptation and online learning when the true risk function itself is not known (since the statistical distribution of the data is not known). Also, our results consider a general multi-agent scenario involving distributed optimization where *each* individual agent employs random coordinates for its own gradient direction, and these coordinates are generally different from the coordinates used by other agents. In other words, the networked scenario adds significant flexibility into the operation of the agents under model (5).

B. Relation to Partial Updating Schemes

It is also important to clarify the differences between our formulation and other works in the literature, which rely on other useful notions of partial information updates. To begin with, our formulation (5) is different from the models used in [16]–[18] where the step-size parameter was modeled as a random Bernoulli variable, $\mu_k(i)$, which could assume the values μ_k or zero with certain probability. In that case, when the step-size is zero, all entries of $\psi_{k,i}$ will not be updated and adaptation is turned off completely. This is in contrast to the current scenario where only a subset of the entries are left without update and, moreover, this subset varies randomly from one iteration to another.

Likewise, the useful work [19] employs a different notion of partial sharing of information by focusing on the exchange of partial entries of the weight estimates themselves rather than on partial entries of the gradient directions. In other words, the partial information used in this work relates to the combination steps (3a) and (3c) rather than to the adaptation step (3b). It also focuses on the special case in which the risks $\{J_k(w)\}$ are quadratic in w . In [19], it is assumed that only a subset of the weight entries are shared (diffused) among neighbors and that the estimate itself is still updated fully. In comparison, the formulation we are considering diffuses all entries of the weight estimates. Similarly, in [20] it is assumed that some entries of the regression vector are missing, which causes changes to the gradient vectors. In order to undo these changes, an estimation scheme is proposed in [20] to estimate the missing data. In our formulation, more generally, a random subset of the entries of the gradient vector are set to zero at each iteration, while the remaining entries remain unchanged and do not need to be estimated.

There are also other criteria that have been used in the literature to motivate partial updating. For example, in [21], the periodic and sequential least-mean-squares (LMS) algorithms are proposed, where the former scheme updates the whole coefficient vector every N -th iteration, with $N > 1$, and the latter updates only a fraction of the coefficients, which are pre-determined, at each iteration. In [22], [23] the weight vectors are partially updated by following a set-membership approach, where updates occur only when the *innovation* obtained from the data exceeds a predetermined threshold. In [23]–[25], only entries corresponding to the largest magnitudes in the regression vector or the gradient vector at each agent are updated. However, such scheduled updating techniques may suffer from non-convergence in the presence of nonstationary signals [26]. Partial update schemes can also be based on dimensionality reduction policies using Krylov subspace concepts [27]–[29]. There are also techniques that rely on energy considerations to limit updates, e.g., [30].

The objective of the analysis that follows is to examine the effect of *random* partial gradient information on the learning performance and convergence rate of adaptive networks for general risk functions. We clarify these questions by adapting the framework described in [2], [3].

Notation: We use lowercase letters to denote vectors, uppercase letters for matrices, plain letters for deterministic variables, and boldface letters for random variables. We also use $(\cdot)^T$ to denote transposition, $(\cdot)^{-1}$ for matrix inversion, $\text{Tr}(\cdot)$ for the trace of a matrix, $\text{diag}\{\cdot\}$ for a diagonal matrix, $\text{col}\{\cdot\}$ for a column vector, $\lambda(\cdot)$ for the eigenvalues of a matrix, $\rho(\cdot)$ for the spectral radius of a matrix, $\|\cdot\|$ for the two-induced norm of a matrix or the Euclidean norm of a vector, $\|x\|_\Sigma^2$ for the weighted square value $x^T \Sigma x$, \otimes for Kronecker product, \otimes_b for block Kronecker product. Besides, we use $p \succ 0$ to denote that all entries of vector p are positive. Moreover, $\alpha = O(\mu)$ signifies that $|\alpha| \leq c|\mu|$ for some constant $c > 0$, and $\alpha = o(\mu)$ signifies that $\alpha/\mu \rightarrow 0$ as $\mu \rightarrow 0$. In addition, the notation $\limsup_{n \rightarrow \infty} a(n)$ denotes limit superior of the sequence $a(n)$.

II. DATA MODEL AND ASSUMPTIONS

Let \mathcal{F}_{i-1} represent the filtration (collection) of all random events generated by the processes $\{w_{k,j}\}$ and $\{\Gamma_{k,j}\}$ at all agents up to time $i-1$. In effect, the notation \mathcal{F}_{i-1} refers to the collection of all past $\{w_{k,j}, \Gamma_{k,j}\}$ for all $j \leq i-1$ and all agents.

Assumption 1: (Conditions on indicator variables). It is assumed that the indicator variables $r_{k,i}(m)$ and $r_{\ell,i}(n)$ are independent of each other, for all ℓ, k, m, n . In addition, the variables $\{r_{k,i}(m)\}$ are independent of \mathcal{F}_{i-1} and $\widehat{\nabla_{w^T} J_k(w)}$ for any iterates $w \in \mathcal{F}_{i-1}$ and for all agents k . \square

Let

$$s_{k,i}(\phi_{k,i-1}) \triangleq \widehat{\nabla_{w^T} J_k}(\phi_{k,i-1}) - \nabla_{w^T} J_k(\phi_{k,i-1}) \quad (13)$$

denote the gradient noise at agent k at iteration i , based on the *complete* approximate gradient vector, $\widehat{\nabla_{w^T} J_k}(w)$. We introduce its conditional second-order moment

$$R_{s,k,i}(w) \triangleq \mathbb{E}[s_{k,i}(w)s_{k,i}^T(w)|\mathcal{F}_{i-1}]. \quad (14)$$

The following assumptions are standard and are satisfied by important cases of interest, such as logistic regression risks or mean-square-error risks, as already shown in [2], [3]. These references also motivate these conditions and explain why they are reasonable.

Assumption 2: (Conditions on gradient noise) [2, pp. 496–497]. It is assumed that the first and fourth-order conditional moments of the individual gradient noise processes satisfy the following conditions for any iterates $w \in \mathcal{F}_{i-1}$ and for all $k, \ell = 1, 2, \dots, N$:

$$\mathbb{E}[s_{k,i}(w)|\mathcal{F}_{i-1}] = 0 \quad (15)$$

$$\mathbb{E}[s_{k,i}(w)s_{\ell,i}^T(w)|\mathcal{F}_{i-1}] = 0, \quad k \neq \ell \quad (16)$$

$$\mathbb{E}[\|s_{k,i}(w)\|^4|\mathcal{F}_{i-1}] \leq \beta_k^4 \|w\|^4 + \sigma_{s,k}^4 \quad (17)$$

almost surely, for some nonnegative scalars β_k^4 and $\sigma_{s,k}^4$. \square

Assumption 3: (Smoothness conditions) [2, pp. 552, 576]. It is assumed that the Hessian matrix of each individual cost function, $J_k(w)$, and the covariance matrix of each individual gradient noise process are locally Lipschitz continuous in a small neighborhood around $w = w^o$ in the following manner:

$$\|\nabla_{w^T}^2 J_k(w^o + \Delta w) - \nabla_{w^T}^2 J_k(w^o)\| \leq \kappa_c \|\Delta w\| \quad (18)$$

$$\|R_{s,k,i}(w^o + \Delta w) - R_{s,k,i}(w^o)\| \leq \kappa_d \|\Delta w\|^\gamma \quad (19)$$

for any small perturbations $\|\Delta w\| \leq \varepsilon$ and for some $\kappa_c \geq 0$, $\kappa_d \geq 0$, and parameter $0 < \gamma \leq 4$. \square

III. MAIN RESULTS: STABILITY AND PERFORMANCE

For each agent k , we introduce the error vectors:

$$\tilde{w}_{k,i} \triangleq w^o - w_{k,i} \quad (20)$$

$$\tilde{\phi}_{k,i} \triangleq w^o - \phi_{k,i} \quad (21)$$

$$\tilde{\psi}_{k,i} \triangleq w^o - \psi_{k,i} \quad (22)$$

We also collect all errors, along with the gradient noise processes, from across the network into block vectors:

$$\tilde{\mathbf{w}}_i \triangleq \text{col}\{\tilde{\mathbf{w}}_{1,i}, \tilde{\mathbf{w}}_{2,i}, \dots, \tilde{\mathbf{w}}_{N,i}\} \quad (23)$$

$$\tilde{\boldsymbol{\psi}}_i \triangleq \text{col}\{\tilde{\boldsymbol{\psi}}_{1,i}, \tilde{\boldsymbol{\psi}}_{2,i}, \dots, \tilde{\boldsymbol{\psi}}_{N,i}\} \quad (24)$$

$$\tilde{\boldsymbol{\phi}}_i \triangleq \text{col}\{\tilde{\boldsymbol{\phi}}_{1,i}, \tilde{\boldsymbol{\phi}}_{2,i}, \dots, \tilde{\boldsymbol{\phi}}_{N,i}\} \quad (25)$$

$$\mathbf{s}_i \triangleq \text{col}\{\mathbf{s}_{1,i}, \mathbf{s}_{2,i}, \dots, \mathbf{s}_{N,i}\} \quad (26)$$

For simplicity, in (26) we use the notation $\mathbf{s}_{k,i}$ to replace the gradient noise $\mathbf{s}_{k,i}(\boldsymbol{\phi}_{k,i-1})$ defined in (13), but note vector \mathbf{s}_i is dependent on the collection of $\{\boldsymbol{\phi}_{k,i-1}\}$ for all k . We further introduce the extended matrices:

$$\mathcal{M} \triangleq \text{diag}\{\mu_1, \mu_2, \dots, \mu_N\} \otimes I_M \quad (27)$$

$$\mathcal{A}_1 \triangleq A_1 \otimes I_M, \mathcal{A}_2 \triangleq A_2 \otimes I_M \quad (28)$$

$$\boldsymbol{\Gamma}_i \triangleq \text{diag}\{\boldsymbol{\Gamma}_{1,i}, \boldsymbol{\Gamma}_{2,i}, \dots, \boldsymbol{\Gamma}_{N,i}\} \quad (29)$$

Note that the main difference between the current work and the prior work in [2] is the appearance of the random matrices $\{\boldsymbol{\Gamma}_{k,i}\}$ defined by (5). In the special case when the random matrices are set to the identity matrices across the agents, i.e., $\{\boldsymbol{\Gamma}_{k,i} \equiv I_M\}$, current coordinate-descent case will reduce to the full-gradient update studied in [2]. The inclusion of the random matrices $\{\boldsymbol{\Gamma}_{k,i}\}$ adds a non-trivial level of complication because now, agents update only random entries of their iterates at each iteration and, importantly, these entries vary randomly across the agents. This procedure adds a rich level of randomness into the operation of the multi-agent system. As the presentation will reveal, the study of the stability and limiting performance under these conditions is more challenging than in the stochastic full-gradient diffusion implementation due to at least two factors: (a) First, the evolution of the error dynamics will now involve a *non-symmetric* matrix (matrix $\mathbf{D}_{11,i}$ defined later in (111)); because of this asymmetry, the arguments of [2] do not apply and need to be modified; and (b) second, there is also randomness in the coefficient matrix for the error dynamics (namely, randomness in the matrix \mathbf{B}'_i defined by (39)). These two factors add nontrivial complications to the stability, convergence, and performance analysis of distributed coordinate-descent solutions, as illustrated by the extended derivations in Appendices A and B. These derivations illustrate the new arguments that are necessary to handle the networked solution of this manuscript. For this reason, in the presentation that follows, whenever we can appeal to a result from [2], we will simply refer to it so that, due to space limitations, we can focus the presentation on the new arguments and proofs that are necessary for the current context. It is clear from the proofs in Appendices A and B that these newer arguments are demanding and not straightforward.

Lemma 1: (Network error dynamics). Consider a network of N interacting agents running the diffusion strategy (3) with the gradient vector replaced by (5). The evolution of the error dynamics across the network relative to the reference vector w^o is described by the following recursion:

$$\tilde{\mathbf{w}}_i = \mathcal{B}_i \tilde{\mathbf{w}}_{i-1} + \mathcal{A}_2^\top \mathcal{M} \boldsymbol{\Gamma}_i \mathbf{s}_i \quad (30)$$

where

$$\mathcal{B}_i \triangleq \mathcal{A}_2^\top (I - \mathcal{M} \boldsymbol{\Gamma}_i \mathcal{H}_{i-1}) \mathcal{A}_1^\top \quad (31)$$

$$\mathcal{H}_{i-1} \triangleq \text{diag}\{\mathbf{H}_{1,i-1}, \mathbf{H}_{2,i-1}, \dots, \mathbf{H}_{N,i-1}\} \quad (32)$$

$$\mathbf{H}_{k,i-1} \triangleq \int_0^1 \nabla_w^2 J_k(w^o - t \tilde{\boldsymbol{\phi}}_{k,i-1}) dt. \quad (33)$$

Proof: Refer to [2, pp. 498–504], which is still applicable to the current context. We only need to set in that derivation the matrix A_o to $A_o = I$, and the vector b to $b = 0_{MN}$. These quantities were defined in (8.131) and (8.136) of [2]. The same derivation will lead to (30)–(33), with the main difference being the appearance now of the random matrix $\boldsymbol{\Gamma}_i$ in (30) and (31). \square

We assume that the matrix product $P = A_1 A_2$ is primitive. This condition is guaranteed automatically, for example, for ATC and CTA scenarios when the network is strongly-connected. This means, in view of the Perron-Frobenius Theorem [2], [3], that P has a single eigenvalue at one. We denote the corresponding eigenvector by p , and normalize the entries of p to add up to one. It follows from the same theorem that the entries of p are strictly positive, written as

$$Pp = p, \quad \mathbb{1}^\top p = 1, \quad p \succ 0 \quad (34)$$

with $\mathbb{1}$ being the vector of size N with all its entries equal to one.

Theorem 1: (Network stability). Consider a strongly-connected network of N interacting agents running the diffusion strategy (3) with the gradient vector replaced by (5). Assume the matrix product $P = A_1 A_2$ is primitive. Assume also that the individual cost functions, $J_k(w)$, satisfy the condition in (2) and that Assumptions 1–2 hold. Then, the second and fourth-order moments of the network error vectors are stable for sufficiently small step-sizes, namely, it holds, for all $k = 1, 2, \dots, N$, that

$$\limsup_{i \rightarrow \infty} \mathbb{E} \|\tilde{\mathbf{w}}_{k,i}\|^2 = O(\mu_{\max}) \quad (35)$$

$$\limsup_{i \rightarrow \infty} \mathbb{E} \|\tilde{\mathbf{w}}_{k,i}\|^4 = O(\mu_{\max}^2) \quad (36)$$

for any $\mu_{\max} < \mu_o$, for some small enough μ_o , where

$$\mu_{\max} \triangleq \max\{\mu_1, \mu_2, \dots, \mu_N\}. \quad (37)$$

Proof: The argument requires some effort and is given in Appendix A. \square

Lemma 2: (Long-term network dynamics). Consider a strongly-connected network of N interacting agents running the diffusion strategy (3) under (5). Assume the matrix product $P = A_1 A_2$ is primitive. Assume also that the individual cost functions satisfy (2), and that Assumptions 1–2 and (18) hold. After sufficient iterations, $i \gg 1$, the error dynamics of the network relative to the reference vector w^o is well-approximated by the following model:

$$\tilde{\mathbf{w}}'_i = \mathcal{B}'_i \tilde{\mathbf{w}}'_{i-1} + \mathcal{A}_2^\top \mathcal{M} \boldsymbol{\Gamma}_i \mathbf{s}_i, \quad i \gg 1 \quad (38)$$

where

$$\mathcal{B}'_i \triangleq \mathcal{A}_2^\top (I - \mathcal{M}\mathbf{\Gamma}_i\mathcal{H}) \mathcal{A}_1^\top \quad (39)$$

$$\mathcal{H} \triangleq \text{diag}\{H_1, H_2, \dots, H_N\} \quad (40)$$

$$H_k \triangleq \nabla_w^2 J_k(w^o) \quad (41)$$

More specifically, it holds for sufficiently small step-sizes that

$$\limsup_{i \rightarrow \infty} \mathbb{E} \|\tilde{\mathbf{w}}'_{k,i}\|^2 = O(\mu_{\max}) \quad (42)$$

$$\limsup_{i \rightarrow \infty} \mathbb{E} \|\tilde{\mathbf{w}}'_{k,i}\|^4 = O(\mu_{\max}^2) \quad (43)$$

$$\limsup_{i \rightarrow \infty} \mathbb{E} \|\tilde{\mathbf{w}}'_i\|^2 = \limsup_{i \rightarrow \infty} \mathbb{E} \|\tilde{\mathbf{w}}_i\|^2 + O(\mu_{\max}^{3/2}). \quad (44)$$

Proof: To establish (38), we refer to the derivation in [2, pp. 553–555], and note that, in our case, $\|\mathbf{\Gamma}_i\| \leq 1$ and $b = 0_{MN}$ (which appeared in (10.2) of [2]). Moreover, the results in (42) and (43) can be established by following similar techniques to the proof of Theorem 1, where the only difference is that the random matrix \mathcal{H}_{i-1} defined in (32) is now replaced with the deterministic matrix \mathcal{H} defined by (40), and by noting that the matrices $\{H_k\}$ in (41) still satisfy the condition (2). With regards to result (44), we refer to the argument in [2, pp. 557–560] and note again that $\|\mathbf{\Gamma}_i\| \leq 1$. \square

Result (35) ensures that the mean-square-error (MSE) performance of the network is in the order of μ_{\max} . Using the long-term model (38), we can be more explicit and derive the proportionality constant that describes the value of the network mean-square-error to first-order in μ_{\max} . To do so, we introduce the quantity

$$q \triangleq \text{diag}\{\mu_1, \mu_2, \dots, \mu_N\} A_2 p \quad (45)$$

and the gradient-noise covariance matrices:

$$G_k \triangleq \lim_{i \rightarrow \infty} \mathbf{R}_{s,k,i}(w^o) \quad (46)$$

$$G'_k \triangleq \mathbb{E}[\mathbf{\Gamma}_{k,i} G_k \mathbf{\Gamma}_{k,i}]. \quad (47)$$

Observe that G_k is the limiting covariance matrix of the gradient noise process evaluated at w^o , and is assumed to be a constant value, while G'_k is a weighted version of it. A typical example for the existence of the limit in (46) is the MSE network, where the covariance matrix of the gradient noise is a constant matrix, which is independent of the time index i [2, p. 372]. It follows by direct inspection that the entries of G'_k are given by:

$$G'_k(m, n) = \begin{cases} (1 - r_k)^2 G_k(m, n), & m \neq n \\ (1 - r_k) G_k(m, m), & m = n. \end{cases} \quad (48)$$

We also define the mean-square-deviation (MSD) for each agent k , and the average MSD across the network to first-order in μ_{\max} — see [2] for further clarifications on these expressions where it is explained, for example, that MSD_k provides the steady-state value of the error variance $\mathbb{E} \|\tilde{\mathbf{w}}_{k,i}\|^2$

to first-order in μ_{\max} :

$$\text{MSD}_k \triangleq \mu_{\max} \left(\lim_{\mu_{\max} \rightarrow 0} \limsup_{i \rightarrow \infty} \frac{1}{\mu_{\max}} \mathbb{E} \|\tilde{\mathbf{w}}_{k,i}\|^2 \right) \quad (49)$$

$$\text{MSD}_{av} \triangleq \frac{1}{N} \sum_{k=1}^N \text{MSD}_k. \quad (50)$$

Likewise, we define the excess-risk (ER) for each agent k as the average fluctuation of the normalized aggregate cost

$$\bar{J}^{\text{glob}}(w) \triangleq \left(\sum_{k=1}^N q_k \right)^{-1} \sum_{k=1}^N q_k J_k(w) \quad (51)$$

with $\{q_k\}$ being entries of the vector q defined by (45), around its minimum value $\bar{J}^{\text{glob}}(w^o)$ at steady state to first-order in μ_{\max} , namely [2, p. 581]:

$$\begin{aligned} \text{ER}_k &\triangleq \mu_{\max} \\ &\times \left(\lim_{\mu_{\max} \rightarrow 0} \limsup_{i \rightarrow \infty} \frac{1}{\mu_{\max}} \mathbb{E} \{ \bar{J}^{\text{glob}}(\mathbf{w}_{k,i}) - \bar{J}^{\text{glob}}(w^o) \} \right). \end{aligned} \quad (52)$$

The average ER across the network is defined by

$$\text{ER}_{av} \triangleq \frac{1}{N} \sum_{k=1}^N \text{ER}_k. \quad (53)$$

By following similar arguments to [2, p. 582], it can be verified that the excess risk can also be evaluated by computing a weighted mean-square-error variance:

$$\text{ER}_k \triangleq \mu_{\max} \left(\lim_{\mu_{\max} \rightarrow 0} \limsup_{i \rightarrow \infty} \frac{1}{\mu_{\max}} \mathbb{E} \|\tilde{\mathbf{w}}_{k,i}\|_{\frac{1}{2}\bar{H}}^2 \right) \quad (54)$$

where \bar{H} denotes the Hessian matrix of the normalized aggregate cost, $\bar{J}^{\text{glob}}(w)$, evaluated at the minimizer $w = w^o$:

$$\bar{H} \triangleq \left(\sum_{k=1}^N q_k \right)^{-1} \sum_{k=1}^N q_k H_k \quad (55)$$

with H_k defined by (41). Moreover, we define the convergence rate as the slowest rate at which the error variances, $\mathbb{E} \|\tilde{\mathbf{w}}_{k,i}\|^2$, converge to the steady-state region. By iterating the recursion for the second-order moment of the error vector, we will arrive at a relation in the following form:

$$\mathbb{E} \|\tilde{\mathbf{w}}_i\|^2 = \mathbb{E} \{ \|\tilde{\mathbf{w}}_{-1}\|_{F^{i+1}}^2 \} + c \quad (56)$$

for some matrix F and constant c , where $\tilde{\mathbf{w}}_{-1}$ denotes the network error vector at the initial time instant. The first-term on the right-hand side corresponds to a transient component that dies out with time, and the second-term denotes the steady-state region that $\mathbb{E} \|\tilde{\mathbf{w}}_i\|^2$ converges to. Then, the convergence rate of $\mathbb{E} \|\tilde{\mathbf{w}}_i\|^2$ towards its steady-state region is dictated by $\rho(F)$ [2, p. 395]. The following conclusion is one of the main results in this work. It shows how the coordinate descent construction influences performance in comparison to the standard diffusion strategy where all entries of the gradient vector are used at each iteration. Following the statement of the result, we illustrate its implications by considering several important cases.

Theorem 2: (MSD and ER performance). Under the same setting of Theorem 1, and assume also that Assumption 3 holds, it holds that, for sufficiently small step-sizes:

$$\begin{aligned} \text{MSD}_{\text{coor},k} &= \text{MSD}_{\text{coor},\text{av}} \\ &= \frac{1}{2} \text{Tr} \left(\left(\sum_{k=1}^N q_k (1-r_k) H_k \right)^{-1} \sum_{k=1}^N q_k^2 G'_k \right) \end{aligned} \quad (57)$$

$$\text{ER}_{\text{coor},k} = \text{ER}_{\text{coor},\text{av}} = \frac{1}{2} \text{Tr} \left(X \sum_{k=1}^N q_k^2 G'_k \right) \quad (58)$$

where the subscript “coor” denotes the stochastic coordinate-descent diffusion implementation, and matrix X is the unique solution to the following Lyapunov equation:

$$X \left(\sum_{k=1}^N q_k (1-r_k) H_k \right) + \left(\sum_{k=1}^N q_k (1-r_k) H_k \right) X = \bar{H} \quad (59)$$

with \bar{H} defined by (55). Moreover, for large enough i , the convergence rate of the error variances, $\mathbb{E} \|\tilde{\mathbf{w}}_{k,i}\|^2$, towards the steady-state region (57) is given by

$$\alpha_{\text{coor}} = 1 - 2\lambda_{\min} \left(\sum_{k=1}^N q_k (1-r_k) H_k \right) + O \left(\mu_{\max}^{(N+1)/N} \right) \quad (60)$$

Proof: See Appendix B. \square

IV. IMPLICATIONS AND USEFUL CASES

A. Uniform Missing Probabilities

Consider the case when the missing probabilities are identical across the agents, i.e., $\{r_k \equiv r\}$.

1) *Convergence time:* Consider the ATC or CTA forms of the full-gradient or coordinate-descent diffusion strategy (3a)–(3c) and (5). From (56), we find that the error variances for the distributed strategies evolve according to a relation of the form:

$$\mathbb{E} \|\tilde{\mathbf{w}}_{k,i}\|^2 \leq \alpha^{i+1} \mathbb{E} \|\tilde{\mathbf{w}}_{k,-1}\|^2 + c \quad (61)$$

for some constant $c > 0$, and where the parameter α determines the convergence rate. Its value is denoted by α_{grad} for the full-gradient implementation and is given by [2, p. 584]:

$$\alpha_{\text{grad}} = 1 - 2\lambda_{\min} \left(\sum_{k=1}^N q_k H_k \right) + o(\mu_{\max}) \quad (62)$$

Likewise, the convergence rate for the coordinate-descent variant is denoted by α_{coor} and is given by expression (60). It is clear that $\alpha_{\text{coor}} \geq \alpha_{\text{grad}}$ for $0 \leq r < 1$, so that the coordinate-descent implementation converges at a slower rate as expected (since it only employs partial gradient information). Thus, let T_{coor} and T_{grad} denote the largest number of iterations that are needed for the error variances, $\mathbb{E} \|\tilde{\mathbf{w}}_{k,i}\|^2$, to converge to their steady-state regions. The values of T_{coor} and T_{grad} can be estimated by assessing the number of iterations that it takes

for the transient term $\alpha^{i+1} \mathbb{E} \|\tilde{\mathbf{w}}_{k,-1}\|^2$ in (61) to assume a higher-order value in μ_{\max} , i.e., for

$$\alpha_{\text{coor}}^{T_{\text{coor}}} \mathbb{E} \|\tilde{\mathbf{w}}_{k,-1}\|^2 = d \mu_{\max}^{1+\epsilon} \quad (63)$$

$$\alpha_{\text{grad}}^{T_{\text{grad}}} \mathbb{E} \|\tilde{\mathbf{w}}_{k,-1}\|^2 = d \mu_{\max}^{1+\epsilon} \quad (64)$$

for some proportionality constant d , and small number $\epsilon > 0$. Then, it holds that

$$\begin{aligned} \frac{T_{\text{coor}}}{T_{\text{grad}}} &= \frac{\ln \alpha_{\text{grad}}}{\ln \alpha_{\text{coor}}} \\ &\stackrel{(a)}{\approx} \frac{\ln \left(1 - 2\lambda_{\min} \left(\sum_{k=1}^N q_k H_k \right) \right)}{\ln \left(1 - 2\lambda_{\min} \left(\sum_{k=1}^N q_k (1-r) H_k \right) \right)} \\ &\stackrel{(b)}{\approx} \frac{-2\lambda_{\min} \left(\sum_{k=1}^N q_k H_k \right)}{-2(1-r)\lambda_{\min} \left(\sum_{k=1}^N q_k H_k \right)} \\ &= \frac{1}{1-r} \end{aligned} \quad (65)$$

where in step (a) we ignored the higher-order term in μ_{\max} , and in (b) we used $\ln(1-x) \approx -x$ as $x \rightarrow 0$. Expression (65) reveals by how much the convergence time is increased in the coordinate-descent implementation. Note that because of longer convergence time, the stochastic coordinate-descent diffusion implementation may require more quantities to be exchanged across the network compared to the full-gradient case.

2) *Computational complexity:* Let us now compare the computational complexity of both implementations: the coordinate-descent and the full-gradient versions. Assume that the computation required to calculate each entry of the gradient vector $\widehat{\nabla_{w^T} J_k}(\phi_{k,i-1})$ is identical, and let $c_m \geq 0$ and $c_a \geq 0$ denote the number of multiplications and additions, respectively, that are needed for each entry of the gradient vector.

Let $n_k \triangleq |\mathcal{N}_k|$ denote the degree of agent k . Then, in the full-gradient implementation, the adaptation step (3b) requires $c_m M + M$ multiplications and $c_a M + M$ additions, while the combination step (3a) or (3c) requires $n_k M$ multiplications and $(n_k - 1)M$ additions. In the coordinate-descent implementation, the adaptation step (3b) with the gradient vector replaced by (5) requires $(1-r) \cdot (c_m M + M)$ multiplications and $(1-r) \cdot (c_a M + M)$ additions on average, while the combination step (3a) or (3c) requires $n_k M$ multiplications and $(n_k - 1)M$ additions. Let $m_{\text{coor},k}$ and $m_{\text{grad},k}$ denote the combined number of multiplications required by the adaptation and combination steps per iteration at each agent k in the coordinate-descent and full-gradient cases. Then,

$$m_{\text{grad},k} = (c_m + n_k + 1)M \quad (66)$$

$$m_{\text{coor},k} = m_{\text{grad},k} - (c_m + 1)Mr \quad (67)$$

If we now consider that these algorithms take T_{coor} and T_{grad} iterations to reach their steady-state regime, then the total number of multiplications at agent k , denoted by $M_{\text{coor},k}$ and

$M_{\text{grad},k}$, are therefore given by

$$M_{\text{coor},k} = m_{\text{coor},k} T_{\text{coor}} \quad (68)$$

$$M_{\text{grad},k} = m_{\text{grad},k} T_{\text{grad}} \quad (69)$$

so that using (65):

$$\frac{M_{\text{coor},k}}{M_{\text{grad},k}} = \frac{m_{\text{coor},k}}{m_{\text{grad},k}} \frac{1}{1-r} \quad (70)$$

Now, the first term on the right hand side satisfies

$$\frac{m_{\text{coor},k}}{m_{\text{grad},k}} = 1 - \frac{c_m + 1}{c_m + n_k + 1} r \quad (71)$$

so that from (70) and (71):

$$1 \leq \frac{M_{\text{coor},k}}{M_{\text{grad},k}} = (1-r)^{-1} \left(1 - \frac{c_m + 1}{c_m + n_k + 1} r \right) \quad (72)$$

since $0 \leq r < 1$. It is clear that when it is costly to compute the gradient entries, i.e., when $c_m \gg n_k$, then $M_{\text{coor},k}$ and $M_{\text{grad},k}$ will be essentially identical. This means that while the coordinate-descent implementation will take longer to converge, the savings in computation per iteration that it provides is such that the overall computational complexity until convergence remains largely invariant (it is not increased). This is a useful conclusion. It means that in situations where computations at each iteration need to be minimal (e.g., when low end sensors are used), then a coordinate-descent variant is recommended and it will be able to deliver the same steady-state performance (to first-order in μ_{\max} , see (78) ahead) with the total computational demand spread over a longer number of iterations. This also means that the complexity and convergence rate measures, when normalized by the number of entries that are truly updated at each iteration, remain effectively invariant. A similar analysis and conclusion holds if we examine the total number of additions (as opposed to multiplications) that are necessary.

3) *MSD performance*: The matrix G'_k defined by (48) can be written as

$$\begin{aligned} G'_k &= (1-r)^2 G_k + ((1-r) - (1-r)^2) \text{diag}\{G_k\} \\ &= (1-r)^2 \left(G_k + \frac{r}{1-r} \text{diag}\{G_k\} \right) \end{aligned} \quad (73)$$

where the term $\text{diag}\{G_k\}$ is a diagonal matrix that consists of the diagonal entries of G_k . Then, the MSD expression (57) gives

$$\begin{aligned} \text{MSD}_{\text{coor},k} &\stackrel{(73)}{=} \frac{1}{2} (1-r) \text{Tr} \left(\left(\sum_{k=1}^N q_k H_k \right)^{-1} \times \right. \\ &\quad \left. \sum_{k=1}^N q_k^2 \left(G_k + \frac{r}{1-r} \text{diag}\{G_k\} \right) \right) \end{aligned}$$

$$\begin{aligned} &= \frac{1}{2} \text{Tr} \left(\left(\sum_{k=1}^N q_k H_k \right)^{-1} \sum_{k=1}^N q_k^2 G_k \right) + \\ &\quad \frac{r}{2} \text{Tr} \left(\left(\sum_{k=1}^N q_k H_k \right)^{-1} \sum_{k=1}^N q_k^2 \text{diag}\{G_k\} \right) - \\ &\quad \frac{r}{2} \text{Tr} \left(\left(\sum_{k=1}^N q_k H_k \right)^{-1} \sum_{k=1}^N q_k^2 G_k \right). \end{aligned} \quad (74)$$

By recognizing that the first item in (74) is exactly the MSD expression for the stochastic full-gradient diffusion case [2, p. 594], which is denoted by “ $\text{MSD}_{\text{grad},k}$ ”, we get

$$\begin{aligned} \text{MSD}_{\text{coor},k} - \text{MSD}_{\text{grad},k} &= \\ &= \frac{r}{2} \text{Tr} \left(\left(\sum_{k=1}^N q_k H_k \right)^{-1} \sum_{k=1}^N q_k^2 \check{G}_k \right) \end{aligned} \quad (75)$$

where

$$\check{G}_k \triangleq \text{diag}\{G_k\} - G_k. \quad (76)$$

We show in Appendix C that the difference in (75) can be positive or negative, i.e., the MSD performance can be better or worse in the stochastic coordinate-descent case in comparison to the stochastic full-gradient case. Recall from (49) that the MSD performance is evaluated to first-order in μ_{\max} . Then, the MSD gap in (75) is to first-order in the step-size parameter. Observe that the missing probability r on the right hand side of that equation is independent of μ_{\max} . It thus follows that

$$\text{Tr} \left(\left(\sum_{k=1}^N q_k H_k \right)^{-1} \sum_{k=1}^N q_k^2 \check{G}_k \right) = O(\mu_{\max}). \quad (77)$$

Corollary 1: (Small missing probabilities). Let $r = O(\mu_{\max}^\varepsilon)$ for a small number $\varepsilon > 0$. It holds that

$$\text{MSD}_{\text{coor},k} - \text{MSD}_{\text{grad},k} = O(\mu_{\max}^{1+\varepsilon}) = o(\mu_{\max}). \quad (78)$$

Proof: It follows from (75) and (77). \square

We proceed to provide a general upper bound for the difference between $\text{MSD}_{\text{coor},k}$ and $\text{MSD}_{\text{grad},k}$.

Corollary 2: (Upper bound). Under the same conditions of Theorem 2, and when the missing probabilities are uniform, namely, $\{r_k \equiv r\}$, it holds that:

$$\begin{aligned} |\text{MSD}_{\text{coor},k} - \text{MSD}_{\text{grad},k}| &\leq \\ &\frac{r}{2} \left(\sum_{k=1}^N q_k \right)^{-1} \left(\frac{1}{\nu_d} - \frac{1}{\delta_d} \right) \sum_{k=1}^N q_k^2 \text{Tr}(G_k) \end{aligned} \quad (79)$$

where the positive numbers $\nu_d \leq \delta_d$ are defined in (2), and the matrices $\{G_k\}$ are defined by (46). Furthermore, when the matrices $\{H_k\}$ or $\{G_k\}$ are diagonal, it follows that

$$\text{MSD}_{\text{coor},k} = \text{MSD}_{\text{grad},k} \quad (80)$$

Proof: See Appendix D. \square

Corollary 3: (Uniform step-sizes). Continuing with the setting of Corollary 2 by assuming now that the step-sizes are uniform across all agents and $A_1 = I$ or $A_2 = I$ (corresponding to either the ATC or CTA formulations). Let

$\{p_k\}$ be entries of the vector p defined by (34). Then, in view of (45) and (34), $q_k = \mu p_k$ and the $\{p_k\}$ add up to one. In this case, the sum of the $\{q_k\}$ is equal to μ and expression (79) simplifies to

$$|\text{MSD}_{\text{coor},k} - \text{MSD}_{\text{grad},k}| \leq \frac{r}{2} \mu \left(\frac{1}{\nu_d} - \frac{1}{\delta_d} \right) \sum_{k=1}^N p_k^2 \text{Tr}(G_k). \quad (81)$$

□

Consider now MSE networks where the risk function that is associated with each agent k is the mean-square-error:

$$J_k(w) = \mathbb{E}(\mathbf{d}_k(i) - \mathbf{u}_{k,i}w)^2 \quad (82)$$

where $\mathbf{d}_k(i)$ denotes the desired signal, and $\mathbf{u}_{k,i}$ is a (row) regression vector. In these networks, the data $\{\mathbf{d}_k(i), \mathbf{u}_{k,i}\}$ are assumed to be related via the linear regression model

$$\mathbf{d}_k(i) = \mathbf{u}_{k,i}w^o + \mathbf{v}_k(i) \quad (83)$$

where $\mathbf{v}_k(i)$ is zero-mean white measurement noise with variance $\sigma_{v,k}^2$ and assumed to be independent of all other random variables. The processes $\{\mathbf{d}_k(i), \mathbf{u}_{k,i}, \mathbf{v}_k(i)\}$ are assumed to be jointly wide-sense stationary random processes. Assume also that the regression data $\{\mathbf{u}_{k,i}\}$ are zero-mean, and white over time and space with

$$\mathbb{E} \mathbf{u}_{k,i}^T \mathbf{u}_{\ell,j} \triangleq R_{u,k} \delta_{k,\ell} \delta_{i,j} \quad (84)$$

where $R_{u,k} > 0$, and $\delta_{k,\ell}$ denotes the Kronecker delta sequence. Consider the case when the covariance matrices of the regressors are identical across the network, i.e., $\{R_{u,k} \equiv R_u > 0\}$. Then, it holds that [2, p. 598]

$$H_k \equiv 2R_u, \quad G_k = 4\sigma_{v,k}^2 R_u. \quad (85)$$

Substituting into (75) we have

$$\begin{aligned} & \text{MSD}_{\text{coor},k} - \text{MSD}_{\text{grad},k} \\ &= r \left(\sum_{k=1}^N q_k \right)^{-1} \left(\sum_{k=1}^N q_k^2 \sigma_{v,k}^2 \right) \text{Tr} (R_u^{-1} \text{diag}\{R_u\} - M) \\ &\geq 0 \end{aligned} \quad (86)$$

where (86) holds because $\text{Tr} (R_u^{-1} \text{diag}\{R_u\}) \geq M$, which can be shown by using the property that $\text{Tr}(X) \text{Tr}(X^{-1}) \geq M^2$ for any $M \times M$ symmetric positive-definite matrix X [31, p. 317], and choosing $X = \text{diag}^{\frac{1}{2}}\{R_u\} R_u^{-1} \text{diag}^{\frac{1}{2}}\{R_u\}$. In the case of MSE networks, by exploiting the special relation between the matrices $\{H_k\}$ and $\{G_k\}$ in (85), we are able to show that the MSD in the stochastic coordinate-descent case is always larger (i.e., worse) than or equal to that in the stochastic full-gradient diffusion case (although by not more than $o(\mu_{\max})$, as indicated by (78)). We are also able to provide a general upper bound on the difference between these two MSDs.

Corollary 4: (MSE networks). Under the same conditions of Corollary 2, and for MSE networks with uniform covariance

matrices, i.e., $\{R_{u,k} \equiv R_u > 0\}$, it holds that

$$0 \leq \text{MSD}_{\text{coor},k} - \text{MSD}_{\text{grad},k} \leq r \left(\sum_{k=1}^N q_k \right)^{-1} \left(\sum_{k=1}^N q_k^2 \sigma_{v,k}^2 \right) \left(\frac{\delta_d}{\nu_d} - 1 \right) M \quad (87)$$

Moreover, it holds that $\text{MSD}_{\text{coor},k} = \text{MSD}_{\text{grad},k}$ if, and only if, R_u is diagonal.

Proof: It follows from Corollary 2 by using $\text{Tr}(G_k) = 4\sigma_{v,k}^2 \text{Tr}(R_u)$ and noting that $\nu_d/2 \leq \lambda(R_u) \leq \delta_d/2$ according to (85) and (2). □

4) *ER performance:* Consider the scenario when the missing probabilities are identical across the agents, i.e., $\{r_k \equiv r\}$. Then, expression (59) simplifies to

$$(1-r) \left(\sum_{k=1}^N q_k \right) X \bar{H} + (1-r) \left(\sum_{k=1}^N q_k \right) \bar{H} X = \bar{H} \quad (88)$$

where we used the equality $\sum_{k=1}^N q_k H_k = \left(\sum_{k=1}^N q_k \right) \bar{H}$, it follows that

$$X = \frac{1}{2} (1-r)^{-1} \left(\sum_{k=1}^N q_k \right)^{-1} I_M. \quad (89)$$

Thus, the ER expression in (58) can be rewritten as:

$$\begin{aligned} \text{ER}_{\text{coor},k} &= \frac{1}{4} (1-r)^{-1} \left(\sum_{k=1}^N q_k \right)^{-1} \text{Tr} \left(\sum_{k=1}^N q_k^2 G'_k \right) \\ &\stackrel{(a)}{=} \frac{1}{4} \left(\sum_{k=1}^N q_k \right)^{-1} \sum_{k=1}^N q_k^2 \text{Tr}(G_k) \end{aligned} \quad (90)$$

which is exactly the same result for the full gradient case from [2, p. 608], and where the equality (a) holds because $\text{Tr}(G'_k) = (1-r) \text{Tr}(G_k)$ according to the definition in (48).

B. Uniform Individual Costs

Consider the case when the individual costs, $J_k(w)$, are identical across the network, namely, [2, p. 610]

$$J_k(w) \equiv J(w) \triangleq \mathbb{E} Q(w; \mathbf{x}_{k,i}) \quad (91)$$

where $Q(w; \mathbf{x}_{k,i})$ denotes the loss function. In this case, it will hold that the matrices $\{H_k, G_k\}$ are uniform across the agents, i.e.,

$$H_k = \nabla_w^2 J(w^o) \equiv H \quad (92)$$

$$G_k = \mathbb{E} \nabla_w^T Q(w^o; \mathbf{x}_{k,i}) [\nabla_w^T Q(w^o; \mathbf{x}_{k,i})]^T \equiv G \quad (93)$$

in view of $\nabla_w^T J(w^o) = 0$. Then, (92) ensures the matrix $\bar{H} = H$ according to the definition in (55). By referring to (59), we have

$$X = \frac{1}{2} \left(\sum_{k=1}^N q_k (1-r_k) \right)^{-1} I_M. \quad (94)$$

Then, expressions (57) and (58) reduce to

$$\begin{aligned} \text{MSD}_{\text{coor},k} &= \text{MSD}_{\text{coor},\text{av}} \\ &= \frac{1}{2} \left(\sum_{k=1}^N q_k (1 - r_k) \right)^{-1} \sum_{k=1}^N q_k^2 \text{Tr}(H^{-1} G'_k) \quad (95) \end{aligned}$$

$$\begin{aligned} \text{ER}_{\text{coor},k} &= \text{ER}_{\text{coor},\text{av}} \\ &= \frac{1}{4} \left(\sum_{k=1}^N q_k (1 - r_k) \right)^{-1} \sum_{k=1}^N q_k^2 (1 - r_k) \text{Tr}(G). \quad (96) \end{aligned}$$

We proceed to compare the MSD and ER performance in the stochastic full-gradient and coordinate-descent cases. Let

$$\alpha \triangleq \frac{\sum_{k=1}^N q_k^2 (1 - r_k)^2}{\sum_{k=1}^N q_k (1 - r_k)} - \frac{\sum_{k=1}^N q_k^2}{\sum_{k=1}^N q_k} \quad (97)$$

$$\theta \triangleq \frac{\sum_{k=1}^N q_k^2 (1 - r_k)}{\sum_{k=1}^N q_k (1 - r_k)} - \frac{\sum_{k=1}^N q_k^2}{\sum_{k=1}^N q_k} \quad (98)$$

and note that $\alpha \leq \theta$, with equality if, and only if, $\{r_k \equiv 0\}$.

Corollary 5: (Performance comparison). Under the same conditions of Theorem 2, when the individual costs $J_k(w)$ are identical across the agents, it holds that:

a) if $\alpha \geq 0$:

$$0 \leq \text{MSD}_{\text{coor},k} - \text{MSD}_{\text{grad},k} \leq \frac{1}{2} \frac{\theta}{\nu_d} \text{Tr}(G) \quad (99)$$

b) if $\alpha < 0$, and $\theta \geq (1 - \delta_d/\nu_d) \alpha \geq 0$:

$$0 \leq \text{MSD}_{\text{coor},k} - \text{MSD}_{\text{grad},k} \leq \frac{1}{2} \left(\frac{\theta}{\nu_d} + \left(\frac{1}{\delta_d} - \frac{1}{\nu_d} \right) \alpha \right) \text{Tr}(G) \quad (100)$$

c) if $\alpha < 0$, and $\theta \leq (1 - \nu_d/\delta_d) \alpha \leq 0$:

$$\frac{1}{2} \left(\frac{\theta}{\delta_d} + \left(\frac{1}{\nu_d} - \frac{1}{\delta_d} \right) \alpha \right) \text{Tr}(G) \leq \text{MSD}_{\text{coor},k} - \text{MSD}_{\text{grad},k} \leq 0. \quad (101)$$

Likewise, it holds that

$$\text{ER}_{\text{coor},k} - \text{ER}_{\text{grad},k} = \frac{\theta}{4} \text{Tr}(G). \quad (102)$$

Then, in the case when either the missing probabilities or the quantities $\{q_k\}$ are uniform across the agents, namely, $\{r_k \equiv r\}$ or $\{q_k \equiv q\}$, it follows that

$$\text{ER}_{\text{coor},k} = \text{ER}_{\text{grad},k}. \quad (103)$$

Proof: See Appendix E. \square

Note that for the other choices of parameter θ that are not indicated in Corollary 5, there is no consistent conclusion on which MSD (between $\text{MSD}_{\text{coor},k}$ and $\text{MSD}_{\text{grad},k}$) is lower.

V. SIMULATION RESULTS

In this section, we illustrate the results by considering MSE networks and logistic regression networks; both settings satisfy condition (2) and Assumptions 1 through 3.

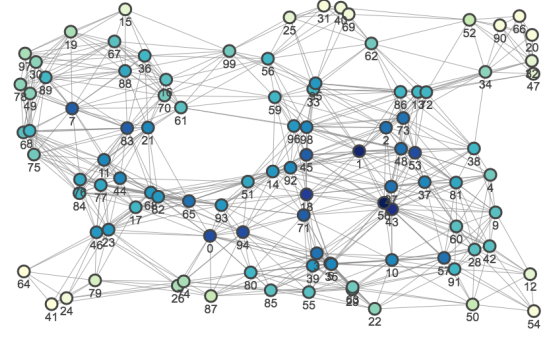


Fig. 1. Network topology consisting of $N = 100$ agents.

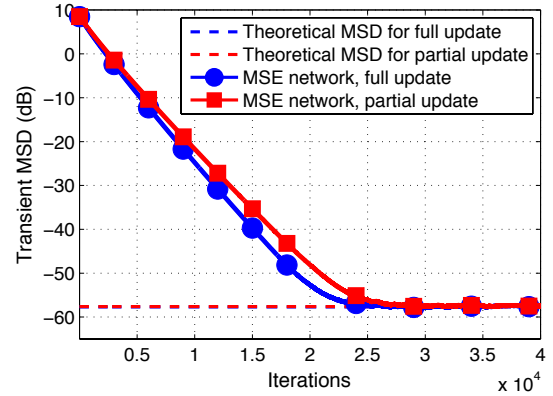


Fig. 2. MSD learning curves, averaged over 200 independent runs, in the case of Corollary 1 when $\{r_k = 0.1\}$. The dashed lines show the theoretical MSD values from (57).

A. MSE Networks

In the following examples, we will test performance of the associated algorithms in the case when uniform missing probabilities are utilized across the agents. We adopt the ATC formulation, and set the combination matrices $A_1 = I$, and A_2 according to the averaging rule [2, p. 664] in the first two examples, and Metropolis rule [2, p. 664] in the third example. In the first example, we test the case when the gradient vectors are missing with small probabilities across the agents. Figure 1 shows a network topology with $N = 100$ agents. The parameter vector w^o is randomly generated with $M = 10$.

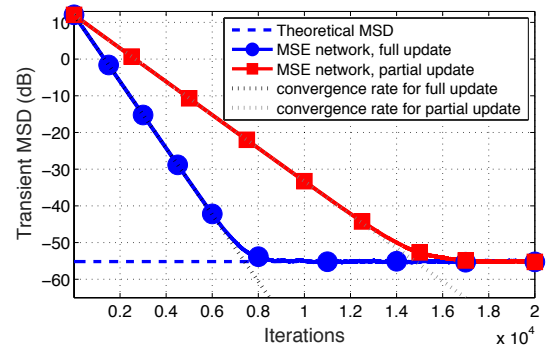


Fig. 3. MSD learning curves, averaged over 200 independent runs, in the case of Corollary 2 when $\{H_k, G_k\}$ are diagonal. The dashed line along the horizontal axis shows the theoretical MSD value from (57). Those along the learning curves show the reference recursion at rates formulated by (60).

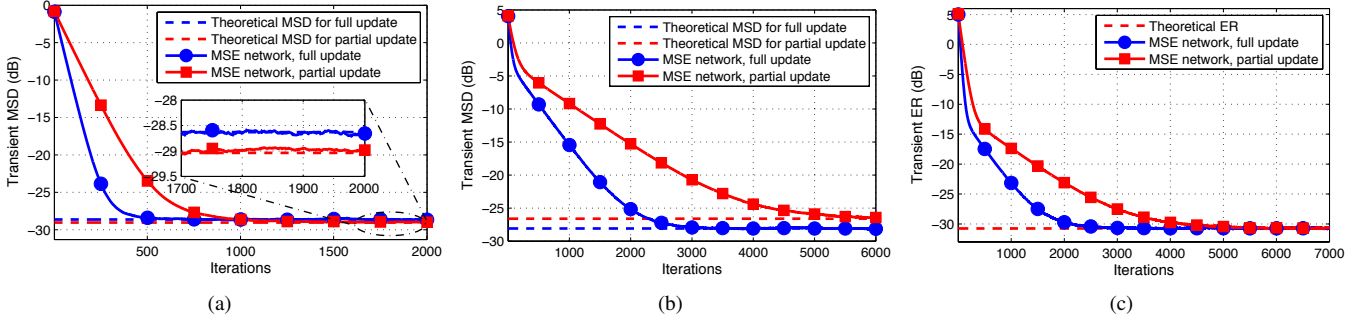


Fig. 4. Learning curves, averaged over 10000 independent runs, and theoretical results calculated from (57) and (58) respectively, for a two-agent MSE network, with parameters $\{\pi_1 = -0.34, \pi_2 = 0.99\}$ in (a), and $\{\pi_1 = 0.34, \pi_2 = 0.99\}$ in (b) and (c).

The regressors are generated by the first-order autoregressive model

$$\mathbf{u}_{k,i}(m) = \pi_k \mathbf{u}_{k,i}(m-1) + \sqrt{1 - \pi_k^2} \mathbf{t}_{k,i}(m), \quad 1 \leq m < M \quad (104)$$

and the variances are scaled to be 1. The processes $\{\mathbf{t}_{k,i}\}$ are zero-mean, unit-variance, and independent and identically distributed (*i.i.d*) Gaussian sequences. The parameters $\{\pi_k\}$ are generated from a uniform distribution on the interval $(-1, 1)$. The noises, uncorrelated with the regression vectors, are zero-mean white Gaussian sequences with the variances uniformly distributed over $(0.001, 0.1)$. The step-sizes $\{\mu_k\}$ across the agents are generated from a uniform distribution on the interval $(0.0001, 0.0005)$. We choose a small missing probability $\{r_k = 0.1\}$. Figure 2 shows the simulation results, which are averaged over 200 independent runs, as well as the theoretical MSD values calculated from (57), which are -57.72dB and -57.61dB , respectively, for the full and partial update case. It is clear from the figure that, when the gradient information is missing with small probabilities, the performance of the coordinate-descent case is close to that of the full-gradient diffusion case.

In the second example, we test the case when the regressors are white across the agents. We randomly generate w^o of size $M = 10$. The white regressors are generated from zero-mean white Gaussian sequences, and the powers, which vary from entry to entry, and from agent to agent, are uniformly distributed over $(0.05, 0.15)$. The noises $\{\mathbf{v}_k(i)\}$, uncorrelated with the regressors, are zero-mean white Gaussian sequences, with the variances $\{\sigma_{v,k}^2\}$ generated from uniform distribution on the interval $(0.0001, 0.01)$. The step-sizes are uniformly distributed over $(0.001, 0.01)$. The results, including the theoretical MSD value from (57) in Theorem 2, the simulated MSD learning curves, and the convergence rates from (60), are illustrated by Fig. 3, where the results are averaged over 200 independent runs. It is clear from the figure that, when white regressors are utilized in MSE networks, the stochastic coordinate-descent case converges to the same MSD level as the full-gradient diffusion case, which verifies (80), at a convergence rate formulated in (60).

In the third example, we revisit the two-agent MSE network discussed in Appendix C, i.e., $N = 2$. We randomly generate w^o of size $M = 2$. The step-sizes $\mu_1 = \mu_2 = 0.005$ are uniform across the agents, which gives $q_1 = q_2 = 2.5 \times$

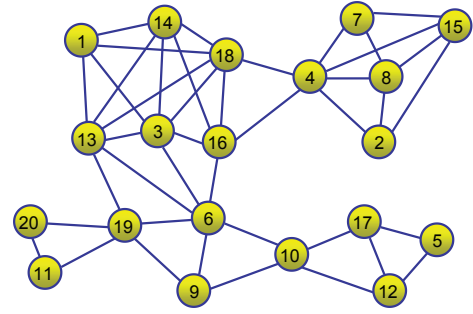


Fig. 5. Network topology consisting of $N = 20$ agents.

10^{-3} . The missing probabilities $r_1 = r_2 = 0.5$. The noises $\{\mathbf{v}_1(i), \mathbf{v}_2(i)\}$ are zero-mean white Gaussian sequences with the variances $\{\sigma_{v,1}^2 = 0.5, \sigma_{v,2}^2 = 5 \times 10^{-4}\}$. The regressors, uncorrelated with the noise sequences, are scaled such that the covariance matrices are of the form

$$R_{u,1} = \begin{bmatrix} |\pi_1| & \pi_1 \\ \pi_1 & 1 \end{bmatrix}, \quad R_{u,2} = \begin{bmatrix} |\pi_2| & \pi_2 \\ \pi_2 & 1 \end{bmatrix} \quad (105)$$

with $|\pi_1| < 1, |\pi_2| < 1$. Now we select parameters $\{\pi_1 = -0.34, \pi_2 = 0.99\}$, which satisfy condition (169a), and $\{\pi_1 = 0.34, \pi_2 = 0.99\}$ to illustrate the cases of $\text{MSD}_{\text{coord},k} < \text{MSD}_{\text{grad},k}$ and $\text{MSD}_{\text{coord},k} > \text{MSD}_{\text{grad},k}$ respectively. Fig. 4 (a) shows the simulation results with the parameters $\{\pi_1 = -0.34, \pi_2 = 0.99\}$. Figures 4 (b) and 4 (c) show the simulation results with the parameters $\{\pi_1 = 0.34, \pi_2 = 0.99\}$. All results are averaged over 10000 independent runs. It is clear from the figures that the simulation results match well with the theoretical results from Theorem 2. In Fig. 4 (a), the steady-state MSD of the stochastic coordinate-descent case is slightly lower than that of the full-gradient diffusion case, by about 0.32dB , which is close to the theoretical MSD difference of 0.41dB from (75). The MSD performance is better in the full-gradient diffusion case in Fig. 4 (b), and the difference between these two MSDs at steady state is 1.71dB , which is close to the theoretical difference of 1.49dB from (75). The ER performance for both the stochastic coordinate-descent and full-gradient diffusion cases are the same as illustrated in Fig. 4 (c), which verifies the theoretical result in (90).

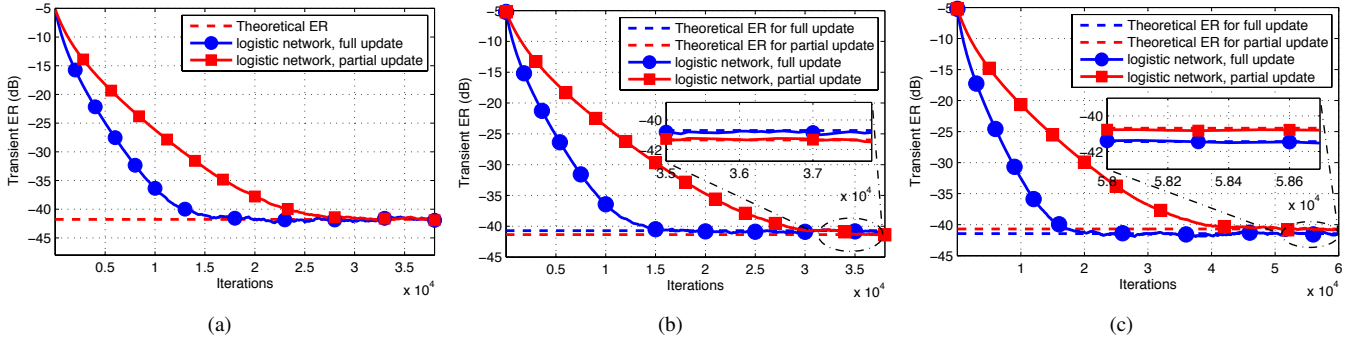


Fig. 6. ER learning curves, averaged over 1000 independent runs, and theoretical results from (96) for diffusion learning over a logistic network with full or partial updates. Corollary 5 is tested in (a) when a uniform step-size and a doubly-stochastic combination matrix are utilized across the network. Corollary 5 is tested when the parameters $\{\mu_k\}$ and $\{r_k\}$ are scaled to make θ in (98) negative in (b) and positive in (c).

B. Logistic Networks

We now consider an application in the context of pattern classification. We assign with each agent the logistic risk

$$J_k(w) = \frac{\rho}{2} \|w\|^2 + \mathbb{E} \left\{ \ln \left[1 + e^{-\gamma_k(i) \mathbf{h}_{k,i}^\top w} \right] \right\} \quad (106)$$

with regularization parameter $\rho > 0$, and where the labels $\{\gamma_k(i) = \pm 1\}$ are binary random and the $\{\mathbf{h}_{k,i}\}$ are feature vectors. The objective is for the agents to determine a parameter vector w^o to enable classification by estimating the class labels via $\hat{\gamma}_k(i) = \mathbf{h}_{k,i}^\top w^o$.

We proceed to test the theoretical findings in Corollary 5. Consider the network topology in Fig. 5 with $N = 20$ agents. We still adopt the ATC formulation, and set the combination matrices $A_1 = I$, and A_2 according to the Metropolis rule in [2, p. 664]. The feature vectors and the unknown parameter vector are randomly generated from uncorrelated zero-mean unit-variance *i.i.d* Gaussian sequences, both of size $M = 10$. The parameter ρ in (106) is set to 0.01. To generate the trajectories for the experiments, the optimal solution to (106), w^o , the Hessian matrix H , and the gradient noise covariance matrix, G , are first estimated off-line by applying a batch algorithm to all data points.

In the first example, we consider the case when a uniform step-size $\{\mu_k = 0.005\}$ is utilized across the agents. All entries of the stochastic gradient vectors are missing completely at random with positive probabilities that are uniformly distributed over $(0, 1)$. Figure 6 (a) shows the transient ER curves for the diffusion strategies with complete and partial gradients, where the results are averaged over 1000 independent runs. The figure also shows the theoretical result calculated from (96). It is clear from Figure 6 (a) that the same ER performance is obtained in the stochastic coordinate-descent and full-gradient diffusion cases, by utilizing a uniform step-size and a doubly-stochastic combination matrix across the agents (in which case the parameters $\{q_k\}$ in (45) are identical across the agents), which is in agreement with the theoretical analysis in (103).

In the second and third examples, we randomly generate the step-sizes $\{\mu_k\}$ and missing probabilities $\{r_k\}$ by following uniform distributions on the intervals $(0.001, 0.01)$ and $(0, 1)$ respectively. In Figure 6 (b), the parameters $\{\mu_k\}$ and $\{r_k\}$

are scaled to get a negative value for θ in (98), and in Fig. 6 (c), those parameters are scaled to make θ positive. Figures 6 (b) and 6 (c) show respectively the transient ER learning curves in these two cases for the diffusion strategies with complete and partial gradients, where the results are averaged over 1000 independent runs. The figures also show the theoretical results calculated from (96). It is clear from Figs. 6 (b) and 6 (c) that these learning curves converge to their theoretical results at steady state. In Fig. 6 (b) where $\theta < 0$, the stochastic coordinate-descent case converges to a lower ER level than the full-gradient diffusion case, and the difference between these two ERs is 0.637dB, which is close to the theoretical difference of 0.640dB from (102). In Fig. 6 (c) where $\theta > 0$, the steady-state ER in the full-gradient diffusion case is lower than that of the stochastic coordinate-descent case, by about 0.726dB, which is close to the theoretical difference of 0.750dB from (102).

APPENDIX A PROOF OF THEOREM 1

Let $P = A_1 A_2$. It was argued in [2, p.510] that P admits a Jordan canonical decomposition of the form $P = V_\epsilon J V_\epsilon^{-1}$ where

$$V_\epsilon \triangleq \begin{bmatrix} p & V_R \end{bmatrix}, V_\epsilon^{-1} \triangleq \begin{bmatrix} \mathbf{1}^\top \\ V_L^\top \end{bmatrix}, J = \begin{bmatrix} 1 & 0 \\ 0 & J_\epsilon \end{bmatrix} \quad (107)$$

p is defined by (34), ϵ denotes an arbitrary positive scalar that we are free to choose, and the matrix J_ϵ has a Jordan structure with ϵ appearing in the first lower diagonal rather than unit entries. All eigenvalues of J_ϵ are strictly inside the unit circle. Then,

$$\mathcal{P} \triangleq P \otimes I_M \triangleq V_\epsilon \mathcal{J} V_\epsilon^{-1} \quad (108)$$

where $V_\epsilon \triangleq V_\epsilon \otimes I_M$, $\mathcal{J} \triangleq J \otimes I_M$. Using (108), we can rewrite \mathcal{B}_i from (31) as

$$\mathcal{B}_i \triangleq (V_\epsilon^{-1})^\top (\mathcal{J}^\top - \mathcal{D}_i^\top) V_\epsilon^\top \quad (109)$$

where

$$\begin{aligned} \mathcal{D}_i^\top &\triangleq V_\epsilon^\top \mathcal{A}_2^\top M \Gamma_i \mathcal{H}_{i-1} \mathcal{A}_1^\top (V_\epsilon^{-1})^\top \\ &= \begin{bmatrix} D_{11,i}^\top & D_{21,i}^\top \\ D_{12,i}^\top & D_{22,i}^\top \end{bmatrix} \end{aligned} \quad (110)$$

and

$$\mathbf{D}_{11,i} = \sum_{k=1}^N q_k \mathbf{H}_{k,i-1} \mathbf{\Gamma}_{k,i} \quad (111)$$

with the vector $q = \{q_k\}$ defined by (45). With regards to the norm of $\mathbf{D}_{11,i}$, we observe that contrary to the arguments in [2, p. 511], this matrix is not symmetric anymore in the coordinate-descent case due to the presence of $\mathbf{\Gamma}_{k,i}$. We therefore need to adjust the arguments, which we do next.

Let

$$\begin{aligned} \bar{\mathbf{D}}_{11,i} &\triangleq \mathbb{E}[\mathbf{D}_{11,i} | \mathcal{F}_{i-1}] \\ &= \sum_{k=1}^N q_k \mathbf{H}_{k,i-1} \mathbb{E}[\mathbf{\Gamma}_{k,i}] \\ &\stackrel{(6)}{=} \sum_{k=1}^N q_k (1 - r_k) \mathbf{H}_{k,i-1} \\ &= \mathbb{E}[\mathbf{D}_{11,i}^\top | \mathcal{F}_{i-1}]. \end{aligned} \quad (112)$$

Noting that

$$\mathbb{E}[\mathbf{\Gamma}_{k,i} \mathbf{\Gamma}_{j,i}] = \begin{cases} (1 - r_k)(1 - r_j), & k \neq j \\ 1 - r_k, & k = j \end{cases} \quad (113)$$

we introduce

$$\begin{aligned} \mathbf{R}_{D_{11,i}} &\triangleq \mathbb{E}[(\mathbf{D}_{11,i} - \bar{\mathbf{D}}_{11,i})(\mathbf{D}_{11,i} - \bar{\mathbf{D}}_{11,i})^\top | \mathcal{F}_{i-1}] \\ &= \mathbb{E}[\mathbf{D}_{11,i} \mathbf{D}_{11,i}^\top | \mathcal{F}_{i-1}] - \bar{\mathbf{D}}_{11,i} \mathbb{E}[\mathbf{D}_{11,i}^\top | \mathcal{F}_{i-1}] - \\ &\quad \mathbb{E}[\mathbf{D}_{11,i} | \mathcal{F}_{i-1}] \bar{\mathbf{D}}_{11,i} + \bar{\mathbf{D}}_{11,i}^2 \\ &\stackrel{(112)}{=} \mathbb{E}[\mathbf{D}_{11,i} \mathbf{D}_{11,i}^\top | \mathcal{F}_{i-1}] - \bar{\mathbf{D}}_{11,i}^2 \\ &= \sum_{k=1}^N \sum_{j=1}^N q_k q_j \mathbf{H}_{k,i-1} \mathbb{E}[\mathbf{\Gamma}_{k,i} \mathbf{\Gamma}_{j,i}] \mathbf{H}_{j,i-1} - \\ &\quad \sum_{k=1}^N \sum_{j=1}^N q_k q_j (1 - r_k)(1 - r_j) \mathbf{H}_{k,i-1} \mathbf{H}_{j,i-1} \\ &\stackrel{(113)}{=} \sum_{k=1}^N \sum_{j \neq k=1}^N q_k q_j (1 - r_k)(1 - r_j) \mathbf{H}_{k,i-1} \mathbf{H}_{j,i-1} - \\ &\quad \sum_{k=1}^N \sum_{j=1}^N q_k q_j (1 - r_k)(1 - r_j) \mathbf{H}_{k,i-1} \mathbf{H}_{j,i-1} + \\ &\quad \sum_{k=1}^N q_k^2 (1 - r_k) \mathbf{H}_{k,i-1}^2 \\ &= \sum_{k=1}^N q_k^2 (1 - r_k) \mathbf{H}_{k,i-1}^2 - \sum_{k=1}^N q_k^2 (1 - r_k)^2 \mathbf{H}_{k,i-1}^2 \\ &= \sum_{k=1}^N q_k^2 (1 - r_k) r_k \mathbf{H}_{k,i-1}^2. \end{aligned} \quad (114)$$

Recall, from (2) and (33), that

$$0 < \nu_d I_M \leq \mathbf{H}_{k,i-1} \leq \delta_d I_M. \quad (116)$$

Then, matrices $\bar{\mathbf{D}}_{11,i}$ and $\mathbf{R}_{D_{11,i}}$ are symmetric positive-definite. Following similar arguments to those in [2, pp. 511–

512], we have

$$\|I_M - \bar{\mathbf{D}}_{11,i}\| \leq 1 - \sigma_{11} \mu_{\max}, \quad \|\mathbf{R}_{D_{11,i}}\| \leq \beta_{11}^2 \mu_{\max}^2 \quad (117)$$

for some positive constants σ_{11} and β_{11}^2 , and sufficiently small μ_{\max} .

Now, multiplying both sides of (30) by $\mathcal{V}_\epsilon^\top$, we have

$$\mathcal{V}_\epsilon^\top \tilde{\mathbf{w}}_i = (\mathcal{J}^\top - \mathcal{D}_i^\top) \mathcal{V}_\epsilon^\top \tilde{\mathbf{w}}_{i-1} + \mathcal{V}_\epsilon^\top \mathcal{A}_2^\top \mathcal{M} \mathbf{\Gamma}_i \mathbf{s}_i \quad (118)$$

where (109) was used. Let

$$\mathcal{V}_\epsilon^\top \tilde{\mathbf{w}}_i = \begin{bmatrix} (p^\top \otimes I_M) \tilde{\mathbf{w}}_i \\ (V_R^\top \otimes I_M) \tilde{\mathbf{w}}_i \end{bmatrix} \triangleq \begin{bmatrix} \bar{\mathbf{w}}_i \\ \tilde{\mathbf{w}}_i \end{bmatrix} \quad (119)$$

$$\mathcal{V}_\epsilon^\top \mathcal{A}_2^\top \mathcal{M} \mathbf{\Gamma}_i \mathbf{s}_i = \begin{bmatrix} (q^\top \otimes I_M) \mathbf{\Gamma}_i \mathbf{s}_i \\ (V_R^\top \otimes I_M) \mathcal{A}_2^\top \mathcal{M} \mathbf{\Gamma}_i \mathbf{s}_i \end{bmatrix} \triangleq \begin{bmatrix} \bar{\mathbf{s}}_i \\ \tilde{\mathbf{s}}_i \end{bmatrix} \quad (120)$$

We then rewrite (118) as

$$\begin{bmatrix} \bar{\mathbf{w}}_i \\ \tilde{\mathbf{w}}_i \end{bmatrix} = \begin{bmatrix} I_M - \mathbf{D}_{11,i}^\top & -\mathbf{D}_{21,i}^\top \\ -\mathbf{D}_{12,i}^\top & \mathcal{J}_\epsilon^\top - \mathbf{D}_{22,i}^\top \end{bmatrix} \begin{bmatrix} \bar{\mathbf{w}}_{i-1} \\ \tilde{\mathbf{w}}_{i-1} \end{bmatrix} + \begin{bmatrix} \bar{\mathbf{s}}_i \\ \tilde{\mathbf{s}}_i \end{bmatrix} \quad (121)$$

where the asymmetry of the matrix $\mathbf{D}_{11,i}$ in this case leads to a difference in the first row, compared to the arguments in [2, pp. 514–515]. We adjust the arguments as follows. Using Jensen's inequality, we have [2, p. 515]:

$$\begin{aligned} \mathbb{E}[\|\bar{\mathbf{w}}_i\|^2 | \mathcal{F}_{i-1}] &\leq \frac{1}{1-t} \mathbb{E}[\|(I_M - \mathbf{D}_{11,i}^\top) \bar{\mathbf{w}}_{i-1}\|^2 | \mathcal{F}_{i-1}] \\ &\quad + \frac{1}{t} \mathbb{E}[\|\mathbf{D}_{21,i}^\top \tilde{\mathbf{w}}_{i-1}\|^2 | \mathcal{F}_{i-1}] + \mathbb{E}[\|\bar{\mathbf{s}}_i\|^2 | \mathcal{F}_{i-1}] \end{aligned} \quad (122)$$

for any $0 < t < 1$, where the expectation of the cross term between $\bar{\mathbf{s}}_i$ and $(I_M - \mathbf{D}_{11,i}^\top) \bar{\mathbf{w}}_{i-1} - \mathbf{D}_{21,i}^\top \tilde{\mathbf{w}}_{i-1}$ vanishes conditioned on \mathcal{F}_{i-1} and $\mathbf{\Gamma}_i$ in view of (15), and the result in (122) follows by taking the expectations again on both sides over $\mathbf{\Gamma}_i$. Then, the first term on the right hand side of (122) can be bounded by

$$\begin{aligned} &\mathbb{E}[\|(I_M - \mathbf{D}_{11,i}^\top) \bar{\mathbf{w}}_{i-1}\|^2 | \mathcal{F}_{i-1}] \\ &= (\bar{\mathbf{w}}_{i-1})^\top \mathbb{E}[(I_M - \mathbf{D}_{11,i})(I_M - \mathbf{D}_{11,i}^\top) | \mathcal{F}_{i-1}] \bar{\mathbf{w}}_{i-1} \\ &\stackrel{(a)}{\leq} \lambda_{\max}(\mathbb{E}[(I_M - \mathbf{D}_{11,i})(I_M - \mathbf{D}_{11,i}^\top) | \mathcal{F}_{i-1}]) \|\bar{\mathbf{w}}_{i-1}\|^2 \\ &\stackrel{(b)}{=} \|\mathbb{E}[(I_M - \mathbf{D}_{11,i})(I_M - \mathbf{D}_{11,i}^\top) | \mathcal{F}_{i-1}]\| \|\bar{\mathbf{w}}_{i-1}\|^2 \\ &\stackrel{(112)}{=} \|I_M - 2\bar{\mathbf{D}}_{11,i} + \mathbb{E}[\mathbf{D}_{11,i} \mathbf{D}_{11,i}^\top | \mathcal{F}_{i-1}]\| \|\bar{\mathbf{w}}_{i-1}\|^2 \\ &\stackrel{(114)}{=} \|I_M - 2\bar{\mathbf{D}}_{11,i} + \bar{\mathbf{D}}_{11,i}^2 + \mathbf{R}_{D_{11,i}}\| \|\bar{\mathbf{w}}_{i-1}\|^2 \\ &\leq (\|(I_M - \bar{\mathbf{D}}_{11,i})^2\| + \|\mathbf{R}_{D_{11,i}}\|) \|\bar{\mathbf{w}}_{i-1}\|^2 \\ &\stackrel{(c)}{=} (\|I_M - \bar{\mathbf{D}}_{11,i}\|^2 + \|\mathbf{R}_{D_{11,i}}\|) \|\bar{\mathbf{w}}_{i-1}\|^2 \\ &\leq ((1 - \sigma_{11} \mu_{\max})^2 + \beta_{11}^2 \mu_{\max}^2) \|\bar{\mathbf{w}}_{i-1}\|^2 \end{aligned} \quad (123)$$

where in step (a) we called upon the Rayleigh-Ritz characterization of eigenvalues [32], [33], and (b), (c) hold because $\|A\| = \lambda_{\max}(A)$ for any symmetric positive-semidefinite matrix A , and $\|A^2\| = \|A\|^2$ for any symmetric matrix A .

Computing the expectations again on both sides of (123),

we have

$$\begin{aligned}
& \frac{1}{1-t} \mathbb{E} \left\{ \mathbb{E} [\| (I_M - \mathbf{D}_{11,i}^\top) \bar{\mathbf{w}}_{i-1} \|^2 | \mathcal{F}_{i-1}] \right\} \\
& \leq \frac{1}{1-t} \left((1 - \sigma_{11} \mu_{\max})^2 + \beta_{11}^2 \mu_{\max}^2 \right) \mathbb{E} \|\bar{\mathbf{w}}_{i-1}\|^2 \\
& \stackrel{(a)}{=} \left(1 - \sigma_{11} \mu_{\max} + \frac{\beta_{11}^2 \mu_{\max}^2}{1 - \sigma_{11} \mu_{\max}} \right) \mathbb{E} \|\bar{\mathbf{w}}_{i-1}\|^2 \\
& \stackrel{(b)}{\leq} (1 - \sigma'_{11} \mu_{\max}) \mathbb{E} \|\bar{\mathbf{w}}_{i-1}\|^2
\end{aligned} \tag{124}$$

where in step (a) we set $t = \sigma_{11} \mu_{\max}$, and in (b) positive number $\sigma'_{11} < \sigma_{11}$, and μ_{\max} is small enough such that $\sigma'_{11} \leq \sigma_{11} - (1 - \sigma_{11} \mu_{\max})^{-1} \beta_{11}^2 \mu_{\max}$. We can now establish (35) by substituting (124) into (122), and completing the argument starting from Eq. (9.69) in the proof of Theorem 9.1 in [2, pp. 516–521], where the quantity $b = 0_{MN}$ (appeared in (9.54) of [2]).

We next establish (36). Compared to the proof for Theorem 9.2 in [2], the main difference, apart from the second-order moments evaluated in (124), is the term

$$\frac{1}{(1-t)^3} \mathbb{E} [\| (I_M - \mathbf{D}_{11,i}^\top) \bar{\mathbf{w}}_{i-1} \|^4] \tag{125}$$

for any $0 < t < 1$, which appeared in (9.117) of [2]. Let

$$\begin{aligned}
\mathbf{K}_i & \triangleq (I_M - \mathbf{D}_{11,i}) (I_M - \mathbf{D}_{11,i}^\top) \bar{\mathbf{w}}_{i-1} (\bar{\mathbf{w}}_{i-1})^\top \\
& \quad \times (I_M - \mathbf{D}_{11,i}) (I_M - \mathbf{D}_{11,i}^\top)
\end{aligned} \tag{126}$$

$$\mathbf{L}_i \triangleq ((I_M - \mathbf{D}_{11,i}) (I_M - \mathbf{D}_{11,i}^\top))^2. \tag{127}$$

Then, both matrices \mathbf{K}_i and \mathbf{L}_i are symmetric positive semi-definite. Thus, we have

$$\begin{aligned}
& \mathbb{E} [\| (I_M - \mathbf{D}_{11,i}^\top) \bar{\mathbf{w}}_{i-1} \|^4 | \mathcal{F}_{i-1}] \\
& = (\bar{\mathbf{w}}_{i-1})^\top \mathbb{E} [\mathbf{K}_i | \mathcal{F}_{i-1}] \bar{\mathbf{w}}_{i-1} \\
& \leq \lambda_{\max} (\mathbb{E} [\mathbf{K}_i | \mathcal{F}_{i-1}]) \|\bar{\mathbf{w}}_{i-1}\|^2 \\
& \stackrel{(a)}{\leq} \text{Tr} (\mathbb{E} [\mathbf{K}_i | \mathcal{F}_{i-1}]) \|\bar{\mathbf{w}}_{i-1}\|^2 \\
& = (\bar{\mathbf{w}}_{i-1}^\top \mathbb{E} [\mathbf{L}_i | \mathcal{F}_{i-1}] \bar{\mathbf{w}}_{i-1}) \|\bar{\mathbf{w}}_{i-1}\|^2 \\
& \leq \lambda_{\max} (\mathbb{E} [\mathbf{L}_i | \mathcal{F}_{i-1}]) \|\bar{\mathbf{w}}_{i-1}\|^4 \\
& = \|\mathbb{E} [\mathbf{L}_i | \mathcal{F}_{i-1}]\| \|\bar{\mathbf{w}}_{i-1}\|^4
\end{aligned} \tag{128}$$

where the inequality (a) holds because $\lambda_{\max}(\Sigma) \leq \text{Tr}(\Sigma)$ for any symmetric positive semi-definite matrix Σ . We proceed to deal with the term $\mathbb{E} [\mathbf{L}_i | \mathcal{F}_{i-1}]$. Note that

$$\mathbf{L}_i = I_M - \mathbf{L}_{1,i} + \mathbf{L}_{2,i} - \mathbf{L}_{3,i} + \mathbf{L}_{4,i} \tag{129}$$

where

$$\mathbf{L}_{1,i} \triangleq 2\mathbf{D}_{11,i} + 2\mathbf{D}_{11,i}^\top \tag{130}$$

$$\mathbf{L}_{2,i} \triangleq 3\mathbf{D}_{11,i} \mathbf{D}_{11,i}^\top + \mathbf{D}_{11,i}^\top \mathbf{D}_{11,i} + (\mathbf{D}_{11,i})^2 + (\mathbf{D}_{11,i}^\top)^2 \tag{131}$$

$$\begin{aligned}
\mathbf{L}_{3,i} & \triangleq (\mathbf{D}_{11,i})^2 \mathbf{D}_{11,i}^\top + \mathbf{D}_{11,i} (\mathbf{D}_{11,i}^\top)^2 + \\
& \quad \mathbf{D}_{11,i} \mathbf{D}_{11,i}^\top \mathbf{D}_{11,i} + \mathbf{D}_{11,i}^\top \mathbf{D}_{11,i} \mathbf{D}_{11,i}^\top
\end{aligned} \tag{132}$$

$$\mathbf{L}_{4,i} \triangleq (\mathbf{D}_{11,i} \mathbf{D}_{11,i}^\top)^2 \tag{133}$$

and we have $\mathbb{E} [\mathbf{L}_{1,i} | \mathcal{F}_{i-1}] = 4\bar{\mathbf{D}}_{11,i}$ according to (112).

Let X be a constant matrix of size $M \times M$. Then,

$$\mathbb{E} [\Gamma_{k,i} X \Gamma_{j,i}] = \begin{cases} (1-r_k)(1-r_j)X, & k \neq j \\ X', & k = j \end{cases} \tag{134}$$

where X' has the same form as (48), and we can further rewrite X' as (73). It follows that:

$$\begin{aligned}
& \mathbb{E} [\mathbf{D}_{11,i}^\top \mathbf{D}_{11,i} | \mathcal{F}_{i-1}] - (\bar{\mathbf{D}}_{11,i})^2 \\
& = \sum_{k=1}^N \sum_{j=1}^N q_k q_j \mathbb{E} [\Gamma_{k,i} \mathbf{H}_{k,i-1} \mathbf{H}_{j,i-1} \Gamma_{j,i} | \mathcal{F}_{i-1}] - \\
& \quad \sum_{k=1}^N \sum_{j=1}^N q_k q_j (1-r_k)(1-r_j) \mathbf{H}_{k,i-1} \mathbf{H}_{j,i-1} \\
& \stackrel{(134)}{=} \sum_{k=1}^N \sum_{j \neq k=1}^N q_k q_j (1-r_k)(1-r_j) \mathbf{H}_{k,i-1} \mathbf{H}_{j,i-1} + \\
& \quad \sum_{k=1}^N q_k^2 (1-r_k)^2 \mathbf{H}_{k,i-1}^2 + \sum_{k=1}^N q_k^2 (1-r_k) r_k \text{diag}\{\mathbf{H}_{k,i-1}^2\} - \\
& \quad \sum_{k=1}^N \sum_{j=1}^N q_k q_j (1-r_k)(1-r_j) \mathbf{H}_{k,i-1} \mathbf{H}_{j,i-1} \\
& = \sum_{k=1}^N q_k^2 (1-r_k) r_k \text{diag}\{\mathbf{H}_{k,i-1}^2\}.
\end{aligned} \tag{135}$$

Recall from (116) that $\{\mathbf{H}_{k,i-1} > 0\}$. Then, $\{\mathbf{H}_{k,i-1}^2 > 0\}$ and $\{\text{diag}\{\mathbf{H}_{k,i-1}^2\} > 0\}$. Computing Euclidean norms on both sides of (135), we have

$$\begin{aligned}
& \|\mathbb{E} [\mathbf{D}_{11,i}^\top \mathbf{D}_{11,i} | \mathcal{F}_{i-1}] - (\bar{\mathbf{D}}_{11,i})^2\| \\
& \stackrel{(a)}{\leq} \sum_{k=1}^N q_k^2 (1-r_k) r_k \|\text{diag}\{\mathbf{H}_{k,i-1}^2\}\| \\
& \stackrel{(b)}{\leq} \sum_{k=1}^N q_k^2 (1-r_k) r_k (\text{Tr}[\mathbf{H}_{k,i-1}^2]) \\
& \leq \sum_{k=1}^N q_k^2 (1-r_k) r_k (M \lambda_{\max}(\mathbf{H}_{k,i-1}^2)) \\
& \stackrel{(116)}{\leq} \sum_{k=1}^N q_k^2 (1-r_k) r_k (M \delta_d^2)
\end{aligned} \tag{136}$$

where in step (a) we used the property that $\|A+B\| \leq \|A\| + \|B\|$ [33], and (b) holds because $\|X\| \leq \text{Tr}(X)$, for any symmetric positive semi-definite matrix X , and that $\text{Tr}[\text{diag}\{X\}] = \text{Tr}[X]$. Recall from (45) that [2, p. 509]

$$q_k = \mu_k (e_k^\top A_2 p) \triangleq \mu_{\max} \tau_k (e_k^\top A_2 p) \tag{137}$$

where e_k denotes the k -th basis vector, which has a unit entry at the k -th location and zeros elsewhere, and the parameter τ_k satisfies $\mu_k = \mu_{\max} \tau_k$. Then, we have

$$\|\mathbb{E} [\mathbf{D}_{11,i}^\top \mathbf{D}_{11,i} | \mathcal{F}_{i-1}] - (\bar{\mathbf{D}}_{11,i})^2\| = O(\mu_{\max}^2) \tag{138}$$

Likewise, it follows that

$$\left\| \mathbb{E} \left[(\mathbf{D}_{11,i})^2 | \mathcal{F}_{i-1} \right] - (\bar{\mathbf{D}}_{11,i})^2 \right\| = O(\mu_{\max}^2) \quad (139)$$

$$\left\| \mathbb{E} \left[(\mathbf{D}_{11,i}^\top)^2 | \mathcal{F}_{i-1} \right] - (\bar{\mathbf{D}}_{11,i})^2 \right\| = O(\mu_{\max}^2). \quad (140)$$

Recall from (117) and (114) that

$$\left\| \mathbb{E} [\mathbf{D}_{11,i} \mathbf{D}_{11,i}^\top | \mathcal{F}_{i-1}] - (\bar{\mathbf{D}}_{11,i})^2 \right\| = O(\mu_{\max}^2). \quad (141)$$

Substituting (138)–(141) into (131), we obtain

$$\left\| \mathbb{E} [\mathbf{L}_{2,i} | \mathcal{F}_{i-1}] - 6 (\bar{\mathbf{D}}_{11,i})^2 \right\| = O(\mu_{\max}^2). \quad (142)$$

Similarly, it can be verified that

$$\left\| \mathbb{E} [\mathbf{L}_{3,i} | \mathcal{F}_{i-1}] - 4 (\bar{\mathbf{D}}_{11,i})^3 \right\| = O(\mu_{\max}^3) \quad (143)$$

$$\left\| \mathbb{E} [\mathbf{L}_{4,i} | \mathcal{F}_{i-1}] - (\bar{\mathbf{D}}_{11,i})^4 \right\| = O(\mu_{\max}^4). \quad (144)$$

It follows that

$$\begin{aligned} \left\| \mathbb{E} [\mathbf{L}_i | \mathcal{F}_{i-1}] \right\| &= \left\| I - \mathbb{E} [\mathbf{L}_{1,i} | \mathcal{F}_{i-1}] + \mathbb{E} [\mathbf{L}_{2,i} | \mathcal{F}_{i-1}] - \right. \\ &\quad \left. \mathbb{E} [\mathbf{L}_{3,i} | \mathcal{F}_{i-1}] + \mathbb{E} [\mathbf{L}_{4,i} | \mathcal{F}_{i-1}] \right\| \\ &= \left\| I - 4 \bar{\mathbf{D}}_{11,i} + 6 (\bar{\mathbf{D}}_{11,i})^2 - 4 (\bar{\mathbf{D}}_{11,i})^3 + \right. \\ &\quad \left. (\bar{\mathbf{D}}_{11,i})^4 + \left(\mathbb{E} [\mathbf{L}_{2,i} | \mathcal{F}_{i-1}] - 6 (\bar{\mathbf{D}}_{11,i})^2 \right) \right. \\ &\quad \left. - \left(\mathbb{E} [\mathbf{L}_{3,i} | \mathcal{F}_{i-1}] - 4 (\bar{\mathbf{D}}_{11,i})^3 \right) \right. \\ &\quad \left. + \left(\mathbb{E} [\mathbf{L}_{4,i} | \mathcal{F}_{i-1}] - (\bar{\mathbf{D}}_{11,i})^4 \right) \right\| \\ &\leq \left\| I - 4 \bar{\mathbf{D}}_{11,i} + 6 (\bar{\mathbf{D}}_{11,i})^2 - 4 (\bar{\mathbf{D}}_{11,i})^3 + \right. \\ &\quad \left. (\bar{\mathbf{D}}_{11,i})^4 \right\| + \left\| \mathbb{E} [\mathbf{L}_{2,i} | \mathcal{F}_{i-1}] - 6 (\bar{\mathbf{D}}_{11,i})^2 \right\| \\ &\quad + \left\| \mathbb{E} [\mathbf{L}_{3,i} | \mathcal{F}_{i-1}] - 4 (\bar{\mathbf{D}}_{11,i})^3 \right\| \\ &\quad + \left\| \mathbb{E} [\mathbf{L}_{4,i} | \mathcal{F}_{i-1}] - (\bar{\mathbf{D}}_{11,i})^4 \right\| \\ &= \left\| (I - \bar{\mathbf{D}}_{11,i})^4 \right\| + O(\mu_{\max}^2) \\ &= \left\| I - \bar{\mathbf{D}}_{11,i} \right\|^4 + O(\mu_{\max}^2) \\ &\stackrel{(117)}{\leq} (1 - \sigma_{11} \mu_{\max})^4 + O(\mu_{\max}^2). \end{aligned} \quad (145)$$

Substituting into (128), and taking expectations again on both sides, we have

$$\begin{aligned} &\frac{1}{(1-t)^3} \mathbb{E} [\| (I_M - \mathbf{D}_{11,i}^\top) \bar{\mathbf{w}}_{i-1} \|^4] \\ &\leq \frac{1}{(1-t)^3} \left((1 - \sigma_{11} \mu_{\max})^4 + O(\mu_{\max}^2) \right) \mathbb{E} \|\bar{\mathbf{w}}_{i-1}\|^4 \\ &\stackrel{(a)}{=} (1 - \sigma_{11} \mu_{\max} + O(\mu_{\max}^2)) \mathbb{E} \|\bar{\mathbf{w}}_{i-1}\|^4 \\ &\leq (1 - \sigma''_{11} \mu_{\max}) \mathbb{E} \|\bar{\mathbf{w}}_{i-1}\|^4 \end{aligned} \quad (146)$$

for some positive constant $\sigma''_{11} < \sigma_{11}$, and for small enough μ_{\max} , where in step (a) we set $t \triangleq \sigma_{11} \mu_{\max}$. Then, the result in (36) can be obtained by continuing from Eq. (9.117) (by choosing $t = \sigma_{11} \mu_{\max}$) in the proof of Theorem 9.2 in [2, pp. 523–530].

APPENDIX B PROOF OF THEOREM 2

Define

$$\mathcal{F} \triangleq \mathbb{E} [\mathcal{B}'_i \otimes_b \mathcal{B}'_i]^\top \quad (147)$$

Then, by following similar techniques shown in the proof of Lemma 9.5 [2, pp. 542–546], we have

$$(I - \mathcal{F})^{-1} = [(p \otimes p)(\mathbf{1} \otimes \mathbf{1})^\top] \otimes Z^{-1} + O(1) \quad (148)$$

where

$$Z \triangleq \sum_{k=1}^N q_k (1 - r_k) [(H_k \otimes I_M) + (I_M \otimes H_k)]. \quad (149)$$

The desired results (57) and (58) in Theorem 2 now follow by referring to the proofs of Theorem 11.2 and Lemma 11.3 in [2, pp. 583–596], and Theorem 11.4 in [2, pp. 608–609].

Evaluating the squared Euclidean norms on both sides of (38) and taking expectations conditioned on \mathcal{F}_{i-1} , then taking expectations again we get

$$\begin{aligned} \mathbb{E} [\|\tilde{\mathbf{w}}'_i\|_{\text{bvec}(I_{NM})}^2] &= \mathbb{E} \left\{ \|\tilde{\mathbf{w}}'_{i-1}\|_{\mathcal{F} \text{bvec}(I_{NM})}^2 \right\} + \\ &\quad \mathbb{E} \left\{ \|\mathbf{s}_i\|_{\mathbb{E}[(\Gamma_i \mathcal{M} \mathcal{A}_2) \otimes_b (\Gamma_i \mathcal{M} \mathcal{A}_2)] \text{bvec}(I_{NM})}^2 \right\} \end{aligned} \quad (150)$$

where we used the weighted vector notation $\|x\|_\sigma^2 = \|x\|_\Sigma^2$ with $\sigma = \text{bvec}(\Sigma)$ and $\text{bvec}(\cdot)$ denoting the block vector operation [2, p. 588]. Iterating the relation we get

$$\begin{aligned} \mathbb{E} [\|\tilde{\mathbf{w}}'_i\|_{\text{bvec}(I_{NM})}^2] &= \mathbb{E} \left\{ \|\tilde{\mathbf{w}}'_{i-1}\|_{\mathcal{F}^{i+1} \text{bvec}(I_{NM})}^2 \right\} + \\ &\quad \sum_{n=0}^i \mathbb{E} \left\{ \|\mathbf{s}_i\|_{\mathbb{E}[(\Gamma_i \mathcal{M} \mathcal{A}_2) \otimes_b (\Gamma_i \mathcal{M} \mathcal{A}_2)] \mathcal{F}^n \text{bvec}(I_{NM})}^2 \right\} \end{aligned} \quad (151)$$

where the first-term corresponds to a transient component that dies out with time, and the convergence rate of $\mathbb{E} \|\tilde{\mathbf{w}}_{k,i}\|^2$ towards the steady-state regime is seen to be dictated by $\rho(\mathcal{F})$ [2, p. 592]. Now, let

$$\Gamma \triangleq \mathbb{E} \Gamma_i = \text{diag}\{(1 - r_k)\}_{k=1}^N \otimes I_M \quad (152)$$

$$\mathcal{M}' \triangleq \mathcal{M} \Gamma = \text{diag}\{\mu_k (1 - r_k)\}_{k=1}^N \otimes I_M \quad (153)$$

$$\mathcal{B}' \triangleq \mathbb{E} \mathcal{B}'_i = \mathcal{A}_2^\top (I - \mathcal{M}' \mathcal{H}) \mathcal{A}_1^\top \quad (154)$$

We now rewrite (147) in terms of \mathcal{B}' as

$$\begin{aligned} \mathcal{F} &\stackrel{(39)}{=} \mathbb{E} [(\mathcal{A}_2^\top (I - \mathcal{M} \Gamma_i \mathcal{H}) \mathcal{A}_1^\top) \otimes_b (\mathcal{A}_2^\top (I - \mathcal{M} \Gamma_i \mathcal{H}) \mathcal{A}_1^\top)]^\top \\ &= (\mathcal{A}_1 \otimes_b \mathcal{A}_1) (I - I \otimes_b (\mathcal{H} \Gamma \mathcal{M}) - (\mathcal{H} \Gamma \mathcal{M}) \otimes_b I + \\ &\quad \mathbb{E} [(\mathcal{H} \Gamma_i \mathcal{M}) \otimes_b (\mathcal{H} \Gamma_i \mathcal{M})]) (\mathcal{A}_2 \otimes_b \mathcal{A}_2) \\ &= [\mathcal{B}' \otimes_b \mathcal{B}']^\top + \Delta_F (\mu_{\max}^2) \end{aligned} \quad (155)$$

where $\Delta_F (\mu_{\max}^2)$ is a matrix whose entries are in the order of $O(\mu_{\max}^2)$. Following similar techniques to the proof of Theorem 9.3 [2, pp. 535–540], we make the same Jordan canonical decomposition for matrix $\mathcal{P} = \mathcal{A}_1 \mathcal{A}_2$ as (108), then substituting into (154) we get

$$\mathcal{B}' = (\mathcal{V}_\epsilon^{-1})^\top (\mathcal{J}^\top - \mathcal{D}'^\top) \mathcal{V}_\epsilon^\top \quad (156)$$

where

$$\begin{aligned} \mathcal{D}'^\top &\triangleq \mathcal{V}_\epsilon^\top \mathcal{A}_2^\top \mathcal{M}' \mathcal{H} \mathcal{A}_1^\top (\mathcal{V}_\epsilon^{-1})^\top \\ &= \begin{bmatrix} D_{11}^{\top} & D_{21}^{\top} \\ D_{12}^{\top} & D_{22}^{\top} \end{bmatrix} \end{aligned} \quad (157)$$

and

$$D'_{11} = \sum_{k=1}^N q_k (1 - r_k) H_k, \quad D'_{21} = O(\mu_{\max}). \quad (158)$$

We now introduce the eigen-decomposition $D'_{11} \triangleq U \Lambda U^T$ for the symmetric positive-definite matrix D'_{11} , where U is unitary, and Λ is a diagonal matrix composed of the eigenvalues of D'_{11} . Let

$$\mathcal{T} = \text{diag}\{\mu_{\max}^{1/N} U, \mu_{\max}^{2/N} I_M, \dots, \mu_{\max}^{(N-1)/N} I_M, \mu_{\max} I_M\} \quad (159)$$

then we have

$$\mathcal{T}^{-1} \mathcal{V}_\epsilon^T \mathcal{B}' (\mathcal{V}_\epsilon^{-1})^T \mathcal{T} = \begin{bmatrix} B'_{11} & B'_{12} \\ B'_{21} & B'_{22} \end{bmatrix}. \quad (160)$$

It follows that $B'_{11} \triangleq I_M - \Lambda$, $B'_{12} = O(\mu_{\max}^{(N+1)/N})$ [2, p. 538]. The matrix \mathcal{B}' has the same eigenvalues as the block matrix on the right hand side of (160). By referring to Gershgorin's Theorem [32], [33], it is shown in [2, pp. 539–540] that the union of the M Gershgorin discs, each centered at an eigenvalue of B'_{11} with radius $O(\mu_{\max}^{(N+1)/N})$, is disjoint from that of the other $M(N-1)$ Gershgorin discs, centered at the diagonal entries of B'_{22} , and therefore

$$\rho(\mathcal{B}') = \rho(B'_{11}) + O(\mu_{\max}^{(N+1)/N}). \quad (161)$$

Let

$$\begin{aligned} \tilde{\Delta}_F &\triangleq (\mathcal{T}^T \mathcal{V}_\epsilon^{-1}) \otimes_b (\mathcal{T}^T \mathcal{V}_\epsilon^{-1}) \Delta_F (\mu_{\max}^2) \times \\ &\quad (\mathcal{V}_\epsilon (\mathcal{T}^{-1})^T) \otimes_b (\mathcal{V}_\epsilon (\mathcal{T}^{-1})^T) \\ &= \begin{bmatrix} O(\mu_{\max}^2) & o(\mu_{\max}^{1/N}) \\ o(\mu_{\max}^2) & \ddots \\ o(\mu_{\max}^{1+1/N}) & O(\mu_{\max}^2) \end{bmatrix}. \end{aligned} \quad (162)$$

It follows from (162) that all the diagonal blocks of $\tilde{\Delta}_F$ are in the order of $O(\mu_{\max}^2)$, the remaining block matrices in the first row are in the order of $o(\mu_{\max}^{1/N})$, the remaining block matrices in the first column are in the order of $o(\mu_{\max}^2)$, and the upper and lower triangular blocks in the $(2, 2)$ th block of $\tilde{\Delta}_F$ are in the order of $o(\mu_{\max}^{2/N})$ and $o(\mu_{\max}^{1+1/N})$ respectively. Then, substituting (160) and (162) into (155), we have

$$\begin{aligned} &(\mathcal{T}^T \mathcal{V}_\epsilon^{-1}) \otimes_b (\mathcal{T}^T \mathcal{V}_\epsilon^{-1}) \mathcal{F} (\mathcal{V}_\epsilon (\mathcal{T}^{-1})^T) \otimes_b (\mathcal{V}_\epsilon (\mathcal{T}^{-1})^T) \\ &= \left(\begin{bmatrix} B'_{11} & B'_{12} \\ B'_{21} & B'_{22} \end{bmatrix} \otimes_b \begin{bmatrix} B'_{11} & B'_{12} \\ B'_{21} & B'_{22} \end{bmatrix} \right)^T + \tilde{\Delta}_F \\ &= \begin{bmatrix} F_{11} & F_{12} \\ F_{21} & F_{22} \end{bmatrix}^T \end{aligned} \quad (163)$$

where

$$F_{11} = B'_{11} \otimes B'_{11} + O(\mu_{\max}^2), \quad F_{12} = O(\mu_{\max}^{(N+1)/N}). \quad (164)$$

Recall that B'_{11} is a diagonal matrix, so is $B'_{11} \otimes B'_{11}$, then we have

$$\text{diag}\{F_{11}\} = \text{diag}\{\lambda(B'_{11} \otimes B'_{11})\} + O(\mu_{\max}^2) \quad (165)$$

which means that the diagonal entries of F_{11} are the eigenvalues of $B'_{11} \otimes B'_{11}$ perturbed by a second-order term, $O(\mu_{\max}^2)$. Referring to Gershgorin's Theorem, the union of the M^2 Gershgorin discs, centered at the diagonal entries of F_{11} with radius $O(\mu_{\max}^{(N+1)/N})$, is disjoint from the union of the other $M^2(N^2-1)$ Gershgorin discs, centered at the diagonal entries of F_{22} . Note that \mathcal{F} has the same eigenvalues as the block matrix on the right hand side of (163), and that eigenvalues are invariant under a transposition operation. It follows from (161) that

$$\rho(\mathcal{F}) = \rho(B'_{11} \otimes B'_{11}) + O(\mu_{\max}^{(N+1)/N}). \quad (166)$$

Using the fact that $\rho(B'_{11} \otimes B'_{11}) = [\rho(B'_{11})]^2$, we arrive at the desired result (60).

APPENDIX C

EXAMINING THE DIFFERENCE IN (75)

We revisit the MSE networks discussed in (82). Assume that there are only two agents in the network as shown in Fig. 7, namely, $N = 2$, with $M = 2$. Assume that $\sigma_{v,1}^2 > \sigma_{v,2}^2$. For

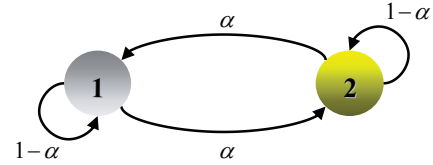


Fig. 7. A two-agent MSE network with a doubly-stochastic combination matrix.

simplicity, uniform parameters $\{q_k \equiv q\}$ are used across the agents (which may occur, for example, in the ATC or CTA forms when the step-sizes are uniform across the agents, i.e., $\{\mu_k \equiv \mu\}$, and doubly-stochastic combination matrices are adopted. In this case, we get $\{q_k \equiv \mu/N\}$ [2, pp. 493–494]). Let

$$R_{u,1} = \begin{bmatrix} |\pi_1| & \pi_1 \\ \pi_1 & 1 \end{bmatrix}, \quad R_{u,2} = \begin{bmatrix} |\pi_2| & \pi_2 \\ \pi_2 & 1 \end{bmatrix} \quad (167)$$

where the numbers $|\pi_1| < 1, |\pi_2| < 1$ ensure that $R_{u,1} > 0, R_{u,2} > 0$. Then, expression (75) can be rewritten as

$$\begin{aligned} &\text{MSD}_{\text{coor},k} - \text{MSD}_{\text{grad},k} \\ &\stackrel{(85)}{=} r q \text{Tr} \left((R_{u,1} + R_{u,2})^{-1} (\sigma_{v,1}^2 (\text{diag}\{R_{u,1}\} - R_{u,1}) + \right. \\ &\quad \left. \sigma_{v,2}^2 (\text{diag}\{R_{u,2}\} - R_{u,2})) \right) \\ &\stackrel{(167)}{=} r q \text{Tr} \left(\begin{bmatrix} |\pi_1| + |\pi_2| & \pi_1 + \pi_2 \\ \pi_1 + \pi_2 & 2 \end{bmatrix}^{-1} \times \right. \\ &\quad \left. \begin{bmatrix} 0 & -\pi_1 \sigma_{v,1}^2 - \pi_2 \sigma_{v,2}^2 \\ -\pi_1 \sigma_{v,1}^2 - \pi_2 \sigma_{v,2}^2 & 0 \end{bmatrix} \right) \\ &= \frac{2 r q (\pi_1 + \pi_2) (\pi_1 \sigma_{v,1}^2 + \pi_2 \sigma_{v,2}^2)}{2 (|\pi_1| + |\pi_2|) - (\pi_1 + \pi_2)^2} \end{aligned} \quad (168)$$

where the denominator is positive for all $|\pi_1| < 1, |\pi_2| < 1$. Then, $\text{MSD}_{\text{coor},k} < \text{MSD}_{\text{grad},k}$ if, and only if $(\pi_1 +$

$\pi_2)(\pi_1\sigma_{v,1}^2 + \pi_2\sigma_{v,2}^2) < 0$, which implies that

$$\begin{cases} 0 < \pi_2 < 1, -\pi_2 < \pi_1 < -(\sigma_{v,2}^2/\sigma_{v,1}^2)\pi_2 & (169a) \\ -1 < \pi_2 < 0, -(\sigma_{v,2}^2/\sigma_{v,1}^2)\pi_2 < \pi_1 < -\pi_2. & (169b) \end{cases}$$

Otherwise, $\text{MSD}_{\text{coor},k} \geq \text{MSD}_{\text{grad},k}$.

APPENDIX D PROOF OF COROLLARY 2

In the case when the matrices $\{H_k\}$ or $\{G_k\}$ are diagonal, it follows from (75) and (76) that $\text{MSD}_{\text{coor},k} - \text{MSD}_{\text{grad},k} = 0$, which verifies (80).

More generally, according to (2) and (46), we have

$$\left(\sum_{k=1}^N q_k H_k\right)^{-1} > 0, \quad \sum_{k=1}^N q_k^2 G_k \geq 0, \quad \sum_{k=1}^N q_k^2 \text{diag}\{G_k\} \geq 0$$

Then, applying the inequality [34]:

$$\lambda_{\min}(A)\text{Tr}(B) \leq \text{Tr}(AB) \leq \lambda_{\max}(A)\text{Tr}(B) \quad (170)$$

for any symmetric positive semi-definite matrices A and B , where $\lambda_{\min}(A)$ and $\lambda_{\max}(A)$ represent respectively the largest and smallest eigenvalues of A , we obtain

$$\begin{aligned} \text{MSD}_{\text{coor},k} - \text{MSD}_{\text{grad},k} &\leq \frac{r}{2} \left\{ \lambda_{\max} \left(\left(\sum_{k=1}^N q_k H_k \right)^{-1} \right) - \right. \\ &\quad \left. \lambda_{\min} \left(\left(\sum_{k=1}^N q_k H_k \right)^{-1} \right) \right\} \sum_{k=1}^N q_k^2 \text{Tr}(G_k) \quad (171) \end{aligned}$$

where we substituted (76) into (75) and used the relation $\text{Tr}(G_k) = \text{Tr}(\text{diag}\{G_k\})$. Then, noting that

$$0 < \sum_{k=1}^N q_k \lambda_{\min}(H_k) \leq \lambda \left(\sum_{k=1}^N q_k H_k \right) \leq \sum_{k=1}^N q_k \lambda_{\max}(H_k) \quad (172)$$

we have

$$\begin{aligned} 1 / \left(\delta_d \sum_{k=1}^N q_k \right) &\stackrel{(a)}{\leq} 1 / \sum_{k=1}^N q_k \lambda_{\max}(H_k) \leq \\ &\lambda \left(\left(\sum_{k=1}^N q_k H_k \right)^{-1} \right) \leq \\ 1 / \sum_{k=1}^N q_k \lambda_{\min}(H_k) &\stackrel{(b)}{\leq} 1 / \left(\nu_d \sum_{k=1}^N q_k \right) \quad (173) \end{aligned}$$

where the inequalities (a) and (b) hold due to (2). Substituting (173) into (171) gives the upper bound for the difference $\text{MSD}_{\text{coor},k} - \text{MSD}_{\text{grad},k}$ as shown by (79). Then, by following a similar argument, we obtain the lower bound for the difference as the opposite number of the upper bound, which leads to the desired result in Corollary 2.

APPENDIX E PROOF OF COROLLARY 5

We start from the MSD expression in (95) and note first that

$$G'_k = (1 - r_k)^2 \left(G + \frac{r_k}{1 - r_k} \text{diag}\{G\} \right) \quad (174)$$

Substituting into (95) we have:

$$\begin{aligned} \text{MSD}_{\text{coor},k} &= \frac{1}{2} \left(\sum_{k=1}^N q_k (1 - r_k) \right)^{-1} \left(\sum_{k=1}^N q_k^2 (1 - r_k)^2 \right) \times \\ &\quad \text{Tr} \left(H^{-1} \left(G + \frac{r_k}{1 - r_k} \text{diag}\{G\} \right) \right) \\ &= \frac{1}{2} \left(\sum_{k=1}^N q_k (1 - r_k) \right)^{-1} \left(\sum_{k=1}^N q_k^2 (1 - r_k)^2 \right) \times \\ &\quad \text{Tr} (H^{-1} G) + \frac{1}{2} \left(\sum_{k=1}^N q_k (1 - r_k) \right)^{-1} \times \\ &\quad \left(\sum_{k=1}^N q_k^2 (1 - r_k) r_k \right) \text{Tr} (H^{-1} \text{diag}\{G\}) \\ &= \frac{1}{2} \left(\sum_{k=1}^N q_k (1 - r_k) \right)^{-1} \left(\sum_{k=1}^N q_k^2 (1 - r_k)^2 \right) \times \\ &\quad \text{Tr} (H^{-1} G) + \frac{1}{2} (\theta - \alpha) \text{Tr} (H^{-1} \text{diag}\{G\}) \quad (175) \end{aligned}$$

where (175) holds because

$$\begin{aligned} \theta - \alpha &= \frac{\sum_{k=1}^N q_k^2 (1 - r_k)}{\sum_{k=1}^N q_k (1 - r_k)} - \frac{\sum_{k=1}^N q_k^2 (1 - r_k)^2}{\sum_{k=1}^N q_k (1 - r_k)} \\ &= \frac{\sum_{k=1}^N q_k^2 (1 - r_k) r_k}{\sum_{k=1}^N q_k (1 - r_k)} \quad (176) \end{aligned}$$

with the numbers α and θ being defined in (97) and (98), respectively. Recall that

$$\text{MSD}_{\text{grad},k} = \frac{1}{2} \left(\sum_{k=1}^N q_k \right)^{-1} \sum_{k=1}^N q_k^2 \text{Tr} (H^{-1} G) \quad (177)$$

is the MSD performance for the full-gradient case. Thus,

$$\begin{aligned} \text{MSD}_{\text{coor},k} - \text{MSD}_{\text{grad},k} &= \frac{1}{2} \left(\frac{\sum_{k=1}^N q_k^2 (1 - r_k)^2}{\sum_{k=1}^N q_k (1 - r_k)} - \frac{\sum_{k=1}^N q_k^2}{\sum_{k=1}^N q_k} \right) \text{Tr} (H^{-1} G) \\ &\quad + \frac{1}{2} (\theta - \alpha) \text{Tr} (H^{-1} \text{diag}\{G\}) \\ &= \frac{\alpha}{2} \text{Tr} (H^{-1} G) + \frac{1}{2} (\theta - \alpha) \text{Tr} (H^{-1} \text{diag}\{G\}). \quad (178) \end{aligned}$$

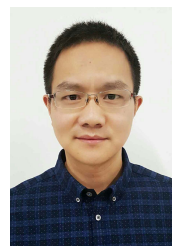
Applying (170) and (2) to (178), we obtain the desired results for the MSD performance shown in Corollary 5. The result for the ER performance in Corollary 5 can be shown by subtracting the ER expression, $\text{ER}_{\text{grad},k}$, on the both sides of (96).

REFERENCES

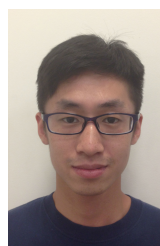
- [1] C. Wang, Y. Zhang, B. Ying, and A. H. Sayed, "Coordinate-descent adaptation over networks," in *Proc. EUSIPCO*, Kos Island, Greece, Aug. 2017.
- [2] A. H. Sayed, "Adaptation, learning, and optimization over networks," *Foundations and Trends in Machine Learning*, vol. 7, no. 4-5, pp. 311–801, 2014.
- [3] A. H. Sayed, "Adaptive networks," *Proceedings of the IEEE*, vol. 102, no. 4, pp. 460–497, Apr. 2014.
- [4] S. Kar, J. M. F. Moura, and K. Ramanan, "Distributed parameter estimation in sensor networks: Nonlinear observation models and imperfect communication," *IEEE Trans. Information Theory*, vol. 58, no. 6, pp. 3575–3605, June 2012.
- [5] A. Nedić and A. Ozdaglar, "Cooperative distributed multi-agent optimization," in *Convex Optimization in Signal Processing and Communications*, D. P. Palomar and Y. C. Eldar, Eds., pp. 340–386. Cambridge University Press, 2010.
- [6] S. Kar and J. M. F. Moura, "Convergence rate analysis of distributed gossip (linear parameter) estimation: Fundamental limits and tradeoffs," *IEEE J. Sel. Top. Signal Process.*, vol. 5, no. 4, pp. 674–690, Aug. 2011.
- [7] A. G. Dimakis, S. Kar, J. M. F. Moura, M. G. Rabbat, and A. Scaglione, "Gossip algorithms for distributed signal processing," *Proc. IEEE*, vol. 98, no. 11, pp. 1847–1864, Nov. 2010.
- [8] S. Sardellitti, M. Giona, and S. Barbarossa, "Fast distributed average consensus algorithms based on advection-diffusion processes," *IEEE Trans. Signal Process.*, vol. 58, no. 2, pp. 826–842, Feb. 2010.
- [9] P. Braca, S. Marano, and V. Matta, "Running consensus in wireless sensor networks," in *Proc. 11th International Conference on Information Fusion*, Cologne, Germany, June 2008, pp. 1–6.
- [10] U. A. Khan and J. M. F. Moura, "Distributing the Kalman filter for large-scale systems," *IEEE Trans. Signal Process.*, vol. 56, no. 10, pp. 4919–4935, Oct. 2008.
- [11] L. Xiao and S. Boyd, "Fast linear iterations for distributed averaging," *Syst. Control Lett.*, vol. 53, no. 1, pp. 65–78, Sep. 2004.
- [12] S.-Y. Tu and A. H. Sayed, "Diffusion strategies outperform consensus strategies for distributed estimation over adaptive networks," *IEEE Trans. Signal Process.*, vol. 60, no. 12, pp. 6217–6234, Dec. 2012.
- [13] Y. Nesterov, "Efficiency of coordinate descent methods on huge-scale optimization problems," *SIAM Journal on Optimization*, vol. 22, no. 2, pp. 341–362, 2012.
- [14] P. Richtárik and M. Takáč, "Iteration complexity of randomized block-coordinate descent methods for minimizing a composite function," *Mathematical Programming*, vol. 144, no. 1-2, pp. 1–38, 2014.
- [15] Z. Lu and L. Xiao, "On the complexity analysis of randomized block-coordinate descent methods," *Mathematical Programming*, vol. 152, pp. 615–642, 2015.
- [16] X. Zhao and A. H. Sayed, "Asynchronous adaptation and learning over networks-Part I: Modeling and stability analysis," *IEEE Trans. Signal Process.*, vol. 63, no. 4, pp. 811–826, Feb. 2015.
- [17] X. Zhao and A. H. Sayed, "Asynchronous adaptation and learning over networks-Part II: Performance analysis," *IEEE Trans. Signal Process.*, vol. 63, no. 4, pp. 827–842, Feb. 2015.
- [18] X. Zhao and A. H. Sayed, "Asynchronous adaptation and learning over networks-Part III: Comparison analysis," *IEEE Trans. Signal Process.*, vol. 63, no. 4, pp. 843–858, Feb. 2015.
- [19] R. Arablouei, S. Werner, Y.-F. Huang, and K. Dogancay, "Distributed least mean-square estimation with partial diffusion," *IEEE Trans. Signal Process.*, vol. 62, no. 2, pp. 472–484, Jan. 2014.
- [20] M. R. Gholami, E. G. Ström, and A. H. Sayed, "Diffusion estimation over cooperative networks with missing data," in *Proc. IEEE GlobalSIP*, Austin, TX, Dec. 2013, pp. 411–414.
- [21] S. C. Douglas, "Adaptive filters employing partial updates," *IEEE Trans. Circuits Syst. II*, vol. 44, no. 3, pp. 209–216, Mar. 1997.
- [22] S. Werner, M. Mohammed, Y.-F. Huang, and V. Koivunen, "Decentralized set-membership adaptive estimation for clustered sensor networks," in *Proc. IEEE ICASSP*, Las Vegas, NV, 2008, pp. 3573–3576.
- [23] S. Werner and Y.-F. Huang, "Time- and coefficient- selective diffusion strategies for distributed parameter estimation," in *Proc. Asilomar Conference on Signals, Systems, and Computers*, Pacific Grove, CA, 2010, pp. 696–700.
- [24] S. C. Douglas, "A family of normalized LMS algorithms," *IEEE Signal Process. Lett.*, vol. 1, no. 3, pp. 49–51, Mar. 1994.
- [25] K. Dogancay, O. Tanrikulu, "Adaptive filtering algorithms with selective partial updates," *IEEE Trans. Circuits Syst. II*, vol. 48, no. 8, pp. 762–769, Aug. 2001.
- [26] M. Godavarti and A. O. Hero, "Partial update LMS algorithms," *IEEE Trans. Signal Process.*, vol. 53, no. 7, pp. 2382–2399, Jul. 2005.
- [27] S. Chouvardas, K. Slavakis, and S. Theodoridis, "Trading off complexity with communication costs in distributed adaptive learning via Krylov subspaces for dimensionality reduction," *IEEE Journal Selected Topics Signal Process.*, vol. 7, no. 2, pp. 257–273, April 2013.
- [28] S. Theodoridis, K. Slavakis, and I. Yamada, "Adaptive learning in a world of projections: A unifying framework for linear and nonlinear classification and regression tasks," *IEEE Signal Process. Magazine*, vol. 28, no. 1, pp. 97–123, Jan. 2011.
- [29] S. Chouvardas, K. Slavakis, Y. Kopsinis, and S. Theodoridis, "A sparsity promoting adaptive algorithm for distributed learning," *IEEE Trans. Signal Process.*, vol. 60, no. 10, pp. 5412–5425, Oct. 2012.
- [30] O. N. Ghahreghshiran, V. Krishnamurthy, and G. Yin, "Distributed energy-aware diffusion least mean squares: Game-theoretic learning," *IEEE J. Sel. Top. Signal Process.*, vol. 7, no. 5, pp. 821–836, Oct. 2013.
- [31] A. H. Sayed, *Adaptive Filters*, Wiley, 2008.
- [32] G. H. Golub and C. F. Van Loan, *Matrix Computations*, The John Hopkins University Press, Baltimore, 3 edition, 1996.
- [33] R. A. Horn and C. R. Johnson, *Matrix Analysis*, Cambridge University Press, 2003.
- [34] Y. Fang, K. A. Loparo, and X. Feng, "Inequalities for the trace of matrix product," *IEEE Trans. Automatic Control*, vol. 39, no. 12, pp. 2489–2490, 1994.



USA. Her research interests include adaptive and statistical signal processing, and distributed adaptation and learning.



interests include signal processing, information fusion and their applications in navigation technology, such as fiber optical gyroscope, inertial navigation and integrated navigation.



Chengcheng Wang (S'17) received the B.Eng. degree in Electrical Engineering and Automation, and Ph.D degree in Control Science and Engineering, from the College of Automation, Harbin Engineering University, Harbin, China, in 2011 and 2017, respectively. She is currently a Research Fellow in the School of Electrical and Electronic Engineering, Nanyang Technological University, Singapore. From Sep. 2014 to Sep. 2016, she was a visiting graduate researcher in Adaptive Systems Laboratory at the University of California, Los Angeles, California, USA.

Yonggang Zhang (S'06–M'07–SM'16) received the B.S. and M.S. degrees from the College of Automation, Harbin Engineering University, Harbin, China, in 2002 and 2004, respectively. He received his Ph.D. degree in Electronic Engineering from Cardiff University, UK in 2007 and worked as a Post-Doctoral Fellow at Loughborough University, UK from 2007 to 2008 in the area of adaptive signal processing. Currently, he is a Professor of Control Science and Engineering in Harbin Engineering University (HEU) in China. His current research

Bicheng Ying (S'15) received his B.S. and M.S. degrees from Shanghai Jiao Tong University (SJTU) and University of California, Los Angeles (UCLA) in 2013 and 2014, respectively. He is currently working towards the PhD degree in Electrical Engineering at UCLA. His research interests include multi-agent network processing, large-scale machine learning, distributed optimization, and statistical signal processing.



Ali H. Sayed (S'90–M'92–SM'99–F'01) is Dean of Engineering at EPFL, Switzerland. He has also served as distinguished professor and former chairman of electrical engineering at UCLA. An author of over 500 scholarly publications and six books, his research involves several areas including adaptation and learning, statistical signal processing, distributed processing, network and data sciences, and biologically-inspired designs. Dr. Sayed has received several awards including the 2015 Education Award from the IEEE Signal Processing Society, the

2014 Athanasios Papoulis Award from the European Association for Signal

Processing, the 2013 Meritorious Service Award, and the 2012 Technical Achievement Award from the IEEE Signal Processing Society. Also, the 2005 Terman Award from the American Society for Engineering Education, the 2003 Kuwait Prize, and the 1996 IEEE Donald G. Fink Prize. He served as Distinguished Lecturer for the IEEE Signal Processing Society in 2005 and as Editor-in-Chief of the IEEE TRANSACTIONS ON SIGNAL PROCESSING (2003–2005). His articles received several Best Paper Awards from the IEEE Signal Processing Society (2002, 2005, 2012, 2014). He is a Fellow of the American Association for the Advancement of Science (AAAS). He is recognized as a Highly Cited Researcher by Thomson Reuters. He is serving as President-Elect of the IEEE Signal Processing Society.